THE UNIVERSITY OF ZAMBIA
SCHOOL OF ENGINEERING
DEPARTMENT OF MECHANICAL ENGINEERING

SIMULATION OF FATIGUE FAILURE IN SISAL AND KENAF REINFORCED POLYPROPYLENE

"FINAL PROJECT REPORT SUBMITTED IN PARTIAL FULFILMENT OF THE REQUIREMENTS FOR THE AWARD OF THE DEGREE OF BACHELOR OF ENGINEERING OF THE UNIVERSITY OF ZAMBIA"

BY

MBIYANA KEEGAN M.

SUPERVISOR: Mr G.M MUNAKAAMPE
CO-SUPERVISOR: Prof S.B KANYANGA
Dr C.K WAMUKWAMBA
Mr C.G CHIZYUK

THE UNIVERSITY OF ZAMBIA
SCHOOL OF ENGINEERING
DEPARTMENT OF MECHANICAL ENGINEERING

SIMULATION OF FATIGUE FAILURE IN SISAL AND KENAF REINFORCED POLYPROPYLENE

"FINAL PROJECT REPORT SUBMITTED IN PARTIAL FULFILMENT OF THE REQUIREMENTS FOR THE AWARD OF THE DEGREE OF BACHELOR OF ENGINEERING OF THE UNIVERSITY OF ZAMBIA"

BY

MBIYANA KEEGAN M.

SUPERVISOR: Mr G.M MUNAKAAMPE
CO-SUPERVISOR: Prof S.B KANYANGA
Dr C.K WAMUKWAMBA
Mr C.G CHIZYUK

DEDICATION

I dedicate this report to my late father and mother, Mr A. Mbiyana and Mrs M. Mbiyana for the support and encouragement during my childhood telling me to believe in myself and for imparting good morals in me, may their souls rest in peace until we meet again.

It is by the grace of the God, I am what I am today and that his grace which was bestowed upon me was not in vain.

ACKNOWLEDGEMENT

Firstly I would like to thank God Almighty for seeing me through my entire education life up to this time.

I wouldn't also forget to acknowledge the significant contribution of my supervisor, Mr G. M. Munakaampe. Without his assistance, guidance, and consistent encouragement, this work wouldn't have reached this far.

Let me also thank Mr C.G Chizyuka the co-supervisor and Mr Kaonga for their assistance in teaching me how to use the software to be used in the project. My sincere gratitude also goes to the members of staff Department of Mechanical Engineering for the opportunity to further my horizon.

Many thanks to my to my uncle Mr F. Mbiyana, elder brother E. Mbiyana and my entire family for the financial and moral support they have been giving me though out my studies.

Lastly but not the least I would like to thank all my classmates for their support and the good friendship.

K. M. Mbiyana

TABLE OF CONTENTS

DEDICATION.....iii

ACKNOWLEDGEMENTS.....iv

TABLE OF CONTENTS.....v

LIST OF FIGURES.....viii

LIST OF TABLES.....x

LIST OF SYMBOLS AND ACRONYMS.....xi

SUMMARY.....xii

CHAPTER ONE: INTRODUCTION

1.1 Background.....1

1.2 Problem Definition.....1

1.3 Objective.....2

1.4 Justification (Rationale).....2

1.5 Scope of work.....3

CHAPTER TWO: LITERATURE REVIEW

2.1 Introduction.....4

2.2 Polymer.....5

2.2.1 Plastic.....6

2.2.2 Classification of plastics.....7

2.2.2.1 Thermoplastic Materials.....7

2.2.2.2 Thermosetting Materials.....8

2.2.3 Polypropylene.....9

2.3 Introduction to Sisal.....9

2.4 Introduction to Kenaf.....16

2.5 Sisal and Kenaf Reinforced polymers.....19

2.6 Fatigue in Natural fibre Reinforced Polymers (NFRP).....21

2.6.1 Fatigue mechanism.....23
2.6.2 Fatigue in plastic.....26
2.6.3 Natural fibre reinforced polymer.....27
2.6.4 Analysis of reinforced plastics.....28
2.6.5 S-N Curves.....28
2.6.6 Fatigue Life Estimation.....29
2.6.7 Statistical nature of fatigue.....29
2.6.8 Effect of mean stress on fatigue.....30
2.7 Design of composite materials and structures.....31
2.7.1 Loading parallel to aligned continuous fibres.....32
2.7.2 Loading perpendicular to aligned continuous fibres.....33
2.7.3 Fibre packing.....36
2.7.3.1 Hexagonal close packing.....36
2.7.3.2 Simple cubic packing.....36
2.7.4 Density, Weight and Volume.....37
2.7.5 Elastic-Brittle, Matrix fail first.....38
2.7.5.1 Loading under constant deflection.....39
2.7.5.2 Loading under constant load.....40
2.7.6 Elastic-Brittle, Fibres break first.....42
2.7.6.1 Loading under constant deflection.....42
2.7.6.2 Loading under constant load.....43

CHAPTER THREE

3.0 METHODOLOGY AND WORK DONE.....45
3.1 Computed physical properties of the composites.....45
3.2 Results from simulations.....47
3.2.1Sisal reinforced polypropylene.....47
3.2.1.1Sisal reinforced polypropylene.....47
3.2.2 Kenaf reinforced polypropylene.....55
3.2.2.1 Simulation results.....55
3.2.3 Fatigue simulation of polyester Lyandenga patience.....64

3.2.4 Fatigue simulation of GFRP Lyandenga patience.....65

CHAPTER FOUR

4.0 DISCUSSION.....68

CHAPTER FIVE

5.0 CONCLUSSION.....70

6.0 RECOMMENDATIONS.....70

REFERENCES.....71

LIST OF FIGURES

Figure 2.3.1 Picture of Sisal plant and Sisal fibres.....10

Figure 2.4.1 Picture of a Kenaf plantation.....18

Figure 2.4.2 Picture of a Kenaf Plant.....19

Figure 2.6.1 Different fatigue loading types.....23

Figure 2.6.2 How fatigue cracks grow.....24

Figure 2.6.3 Crack growth mechanism.....24

Figure 2.6.4 How cracks form in high-cycle fatigue.....25

Figure 2.6.5 How cracks grow in low cycle fatigue.....26

Figure 2.6.2.1 Fatigue behaviour in polymer.....27

Figure 2.6.5.1 Fatigue curve for non-ferrous metals.....28

Figure 2.6.6.1 Life prediction for various amplitude loadings.....29

Figure 2.6.8.1 The combination of properties which maximise the stiffness to weight ratio and strength to weight ratio, for various loading geometries.....30

Figure 2.7.1.1 Composite loaded parallel to aligned fibres.....32

Figure 2.7.2.1 Composite loaded perpendicular to aligned fibres.....34

Figure 2.7.3.1.1 Hexagonal close packing in composites.....36

Figure 2.7.3.2.1 The simple cubic packing in composites.....36

Figure 2.7.5.1 Stress-strain curve for an Elastic-Brittle composite were the matrix fails first.....38

Figure 2.7.5.1.1 Stress-strain curve for an Elastic-Brittle composite loaded under constant deflection.....39

Figure 2.7.5.2.1 Stress- strain curve of a composite loaded under constant load.....40

Figure 2.7.5.2.2 Stress-strain curve of a composite as a function of volume fraction of the fibres.....41

Figure 2.7.6.1 Stress-strain curve for an Elastic-Brittle composite were the fibres fail first.....42

Figure 2.7.6.1.1 Stress-strain curve of a composite loaded under constant deflection..43

Figure 2.7.6.2.1 Stress-strain curve of a composite loaded under constant load.....43

LIST OF TABLES

Table 2.2.2.1 Mechanical properties of thermoplastics and thermosetting materials.....8

Table 2.3.1 Variation of tensile properties of sisal fibre with test length (diameter of fibre: 200μm.....13

Table 2.3.2 Variation of tensile properties of sisal fibre with speed of testing (d= 200μm; length: 50mm).....13

Table 2.3.4 World sisal production.....15

Table 2.5.1 Comparison data between Glass and Kenaf reinforced PP..... 21

Table 3.1.1 Table showing the mechanical properties of polypropylene, sisal and kenaf.....45

Table 3.1.2 Computed mechanical properties of sisal and kenaf composites at different volume fractions.....47

Table 3.2.1.1.1 Physical properties of Sisal reinforced polypropylene with f=0.2.....48

Table 3.2.1.1.2 Mass and Volume of the model used.....48

Table 3.2.1.1.3 Restraint and load.....48

Table 3.2.1.1.4 Mesh and solver information.....49

Table 3.2.1.1.5 Maximum and minimum stresses and their location on the model.....49

Table 3.2.1.1.6 Maximum and minimum strains and their location on the model.....50

Table 3.2.1.1.8 S-N curve, fatigue loading and some fatigue study properties.....52

Table 3.2.1.1.9 Alternating stress vs. number of cycles data points.....53

Table 3.2.1.1.10 Damage, factor of safety, the Biaxiality indicator and life plot.....53

Table 3.2.2.1.1 Physical properties of kenaf reinforced polypropylene with f=0.2.....55

Table 3.2.2.1.9 Alternating stress vs. number of cycles data points.....60

Figure 3.2.1.1.6 Damage factor of safety, the Biaxiality indicator and life plot.....61

LIST OF SYMBOLS AND ACRONYMS

NFRP - Natural fibre reinforced polymer

PP - Polypropylene

FG - Fibre Glass

ABS - Acrylonitrile-Butadiene-Styrene)

PE - Polyethylene

PVC - Polyvinyl chloride

PS - Polystyrene

FG - Fibre Glass

σ_m - Mean Stress

σ_{max} - Maximum Stress

σ_{min} - Minimum Stress

σ_a - Alternating Stress

S - Stress

N - Number of cycles to failure

R - Stress ratio

S-N - Stress-Number of cycles

f - Fibre volume fraction

SUMMARY

Currently Fibre-Glass (FG) is the most widely used reinforcement in polymer composites. However, GF or fibre grass is very expensive and non-biodegradable hence the need for alternative reinforcement materials that are less expensive like natural fibres. Natural fibre reinforced polymers (NFRPs) are widely used in engineering. Products of NFRPs include garden hoses in which the polymer matrix is reinforced with cotton. Like any other engineering material, however, NFRPs could fail due to fatigue. This occurs under repeated or cyclic loading. While the tensile behaviour of these polymers has been investigated to some fair extent, very little has been done on the investigation of fatigue behaviour in natural fibres like sisal and Kenaf as well as their polymer composites

This project is aimed at simulating the failure of natural fibre reinforced polymers (NFRPs) due to fatigue using CosmosWorks, sisal and kenaf in particular. This project will run parallel with another project for SILUMBWE SYDNEY in which actual tests will be done to determine fatigue failure. At the end of the project, the results will assist Engineers to predict fatigue failure in NFRPs and recommend suitable applications of these composites. This will be done by inputting material physical properties into the software and then run the fatigue failure simulation.

CHAPTER ONE

1.0 INTRODUCTION

1.1 Background

The composite industry is quiet new. It has however, grown rapidly in the last few years with the development of fibrous composites like glass-fibre reinforced polymers (fibre-glass) and more recently, carbon-fibre reinforced polymer (CFRP) and natural fibre reinforced polymers (NFRPs). But using the high strength of fibres to stiffen and strengthen a weak, and mostly cheaper, matrix material is probably older than the wheel. The processional way in ancient Babylon, one of the lesser wonders of the ancient world, was made of bitumen reinforced with plaited straw. Straw and horse hair, have been used to reinforce mud bricks (improving their fracture toughness) for at least 5000 years. Paper is a composite, so is concrete; both were known to the Romans. And almost all the natural materials which must bear load- wood, bone, muscle- are composites. (Ashby and Jones, 1995)

NFRPs are widely used in engineering. Products of NFRPs include garden hoses in which the polymer matrix is reinforced with cotton. Like any other engineering material, however, NFRPs could fail due to fatigue. This occurs under repeated or cyclic loading. While the tensile behaviour of these polymers has been investigated to some fair extent, their fatigue behaviour is still the subject of on-going research.

1.2 Problem Definition

At present Glass Fibre (GF) is the most widely used reinforcement in polymer composites. However, GF or fibre grass is very expensive and non-biodegradable hence the need for alternative reinforcement materials that are less expensive like natural fibres. Very little has been done on the investigation of fatigue behavior in natural fibres like sisal, Kenaf and others as well as their polymer composites.

1.3 Projects Objective

The objective of this study were to simulate fatigue failure in NFRPs (sisal and kenaf) using CosmosWorks. To achieve the project's aim, the following were done;

- Studied the tensile and fatigue behaviour of sisal and kenaf and those of polymers in general and polypropylene in particular.
- Studied fatigue failure in polymers in general and NFRP in particular
- Studied and understood Cosmos Works.
- Modeled the fatigue phenomenon in NFRP (Sisal and Kenaf) using CosmosWorks and ran some simulations.
- Comparing simulation results with experimental results from another student SILUMBWE SYDNEY 2010.
- Analysed the results and came up with the required models to predict fatigue failure.
- Wrote a report.

1.4 Justification.

NFRPs just like any other engineering materials could fail due to fatigue. For most of the engineering materials extensive simulations and tests of fatigue have been done and results are readily available in the public domain, while for NFRPs particularly sisal and kenaf, fatigue research is still in its infancy. Sisal and Kenaf can readily be available in Zambia as the conditions for their cultivation are favourable due to good climate and the availability of good arable soils. So there is need to simulate failure in NFRPs due to fatigue.

This project ran parallel with another project in which actual tests were done to determine fatigue failure. This project covers simulation only and its results were to be compared with those obtained from the experimental project.

The results from this project can assist Engineers to predict fatigue failure in NFRPs and recommend suitable applications of these composites.

1.5 Scope of work

This report presents the scope of work done on the simulation of fatigue failure in Natural fibre reinforced polymers.

CHAPTER TWO

2.0 LITERATURE REVIEW

2.1 Introduction

Production of polymer composites has been rocketing worldwide. Production waste is significant but waste management seems to be the most serious problem, hence producers tend to use natural materials which are environmental friendly because they are biodegradable. Application of natural fibres as reinforcing materials is a good idea based on ecological considerations and that the inclusion of fibre reinforcement in polymers can enhance many of the engineering properties of the basic materials, such as fracture toughness, flexural strength and resistance to fatigue, impact, thermal shock and spalling, but it also has other advantages. (Zoltán Mezey, 2002)

Since natural fibres cost less than any other fibres utilized in the industry, the price of the product made of them is also much favourable. Due to the increasing economical and environmental requirements towards the reinforcing materials of load-bearing plastic structural elements, researchers are forced to develop stronger reinforcing materials, reinforcing systems. For instant combining Kenaf fibre with other resources provides a strategy for producing advanced composite materials that take advantage of the properties of both types of resources. It allows the scientist to design materials based on end-use requirements within a framework of cost, availability, recyclability, energy use, and environmental considerations. Kenaf fibres are potentially outstanding reinforcing filler in thermoplastic composites. The specific tensile and flexural moduli, for example, of a 50% by volume of kenaf-polypropylene (PP) composite compares favorably with a 40% by weight of glass fibre PP injection molded composite (But glass fibre is comparatively very expensive). Results indicate that Kenaf fibres are a viable alternative to inorganic/mineral-based reinforcing fibres as long as the right processing conditions and aids are used, and for applications where the higher water absorption of the lignocellulosic-based fibre composite is not critical. (Roger M. Rowell, Anand Sanadi, Rod Jacobson, and Dan Caulfield 1996)

This is why intensive research has started all over the world for the past years, in order to examine the possibility of building different environment-friendly organic and inorganic reinforcing fibres into polymer matrix. Thus, apart from the traditional glass- and carbon fibre reinforcement, new solutions appeared, such as natural fibres (sisal, Kenaf, hemp, tropical plants, e.g. oil palm, coconut, pineapple etc.) or composites containing mineral reinforcing fibres (basalt and ceramics). (Zoltán Mezey, 2002)

2.2 Polymers

Polymers are better known to the general public as plastics, but it is a misnomer to term all polymers as plastics. Polymers are generally classified into three categories; thermoplastic polymers, thermosetting polymers and elastomers, better known as rubbers. Polymers are noted for their low density and their use as insulators - both thermal and electrical. They are poor reflectors of light, tending to be transparent or translucent often in thin sections. Some of them are flexible and subject to deformation. (Lyandenga Patience, 2007)

Polymers contain nonmetallic elements sharing electrons to build up large molecules, called macromolecules. These large molecules contain many repeating units, or mers, from which is obtained the term polymers. By using the term polymer, one often means organic polymers. Basic ingredients of polymers such as ethylene and naphtha are but two of the many products obtained in the cracking of crude oil. (Lyandenga Patience, 2007)

The process of linking together of monomers is called polymerisation. The need to start with the process of polymerisation lies in the necessity of breaking the double bond (C=C) of the monomer. The repeating units of some polymer chains are identical, as in polyethylene, polystyrene and polyvinyl chloride; these repeating units are termed homopolars. Copolymers contain two different types of monomers such as polyvinyl chloride mixed with vinyl acetate to produce polyvinyl acetate; terpolymers such as ABS (Acrylonitrile-Butadiene-Styrene) contain three types of monomers. Polymerisation mechanism may be of the following two types: Addition and condensation polymerisation. (Rajput, 2004)

Addition polymerisation is the simpler of the two. The large molecules are chemically added together by the use of heat and pressure in an autoclave, double bonds of unsaturated monomers break down and then link up into a chain. These addition reactions are atoms or group of atoms that attach themselves to the carbon atom at the sites of multiple bonds. Such a polymerisation takes place in three steps, namely.

- Initiation
- Chain propagation
- Termination

(Rajput, 2004)

Condensation polymerisation is defined as the process of linking together of unlike monomers accompanied by splitting of a small molecule. It yields a by-product which is mostly water and the reaction normally takes hours and/or days. (Rajput, 2004)

2.2.1 Plastic

A plastic can be broadly defined as any non-metallic material that can be moulded to desired shape or they are natural or synthetic resins, or their compounds, which can be moulded, extruded, cast or used as films or coatings. The basic raw materials for producing plastics are from coal, petroleum, limestone, salt, sulphur, air, water and cellulose from cotton and wood. A molding composition for plastics is prepared from the following raw material groups;

Binder: These may be either resins or cellulose derivatives; chemically both kinds of materials may be described as substances made of compounds of very large molecular weight. (Rajput, 2004)

Fillers: These are materials added to the plastic to improve its mechanical properties and to make it economical. These are powder, fibrous, and laminated fillers.

Plasticisers: These chemicals are added to plastics to make them soft; to improve their toughness at finished stage and to make them flexible. A plasticiser should be chemically inert, non-volatile and non-toxic.

Colouring matter: This is usually in the form of pigments and dyes and often added to monomers and gives the required colour to plastics. The colouring matter should be durable and adequately fast to light. Commonly used dyes are organic (AZO dyes) and mineral pigments (chromium oxide).

Lubricants: They facilitate molding operation by increasing the flow of the plastic mix in the die and also to prevent sticking of the plastic to the moulds. Common lubricants are mosallic soaps and stearates.

Catalysts: These compounds are added to accelerate the chemical reaction during the process of polymerisation of plastics. These compounds also act as hardeners. (Rajput, 2004)

2.2.2 Classification of plastics.

Most commonly, plastics are classified into two groups thus Thermoplastics and Thermosetting plastics.

2.2.2.1 Thermoplastic materials

In thermoplastic materials the long chain-like molecules are held together by relatively weak van der waals forces. A useful image of the structure is a mass of randomly distributed long strands of sticky wool. When the material is heated the intermolecular forces are weakened so that it becomes soft and flexible and eventually, at high temperatures, it is a viscous melt. When the material is allowed to cool it solidifies again. This cycle of softening by heat and solidifying when cooled can be repeated more or less indefinitely and is a definite advantage in that it is the basis of most processing methods for these materials, it does have its drawbacks, however, because it means that the properties of thermoplastics are heat sensitive. A useful analogy which is often used to describe these materials is that like candle wax they can be repeatedly softened by heat and will solidify when cooled. Examples of thermoplastics are polyethylene and polyvinyl chloride. (Rajput 2004)

2.2.2.2 Thermosetting materials

A thermosetting material is produced by a chemical reaction which has two stages. The first stage results in the formation of long chain-like molecules similar to those present in thermoplastics, but still capable of further reaction. The second stage of the reaction takes place during molding, usually under the application of heat and pressure. The resultant molding will be rigid when cooled but a close network structure has been set up within the material. During the second stage the long molecular chains have been interlinked by strong bonds so that the material cannot be softened again by the application of heat. If excess heat is applied to these materials they will char and degrade. This type of behavior is analogous to boiling an egg. Once the egg has cooled and is hard, it cannot be softened again by the application of heat. Examples of thermosetting plastics are phenol formaldehyde, melamine formaldehyde and polyester. Table 2.2.2.1 below shows the mechanical properties of thermoplastics and thermosetting materials. (Rajput 2004)

Table 2.2.2.1 Mechanical properties of thermoplastics and thermosetting materials

	Thermoplastics	**Thermosetting**
Properties	Polystyrene	Polyesters
Density(kg/m^3)	1040	1100
Softening point (^oc)	82-103	
Thermal conductivity(W/mK)	0.09-0.21	0.17-0.19
Thermal expansion(/K)	0.00006-0.00008	0.0001-0.00005
Specific heat capacity(J/kgm)	1340-1466	1260
Tensile strength (MN/m^2)	35-62	31-70
Compressive strength (MN/m^2)	90-110	90-240
Young's modulus (MN/m^2)	2410-4130	2800-7000

Source: Rajput 2004

2.2.3 Polypropylene

Polypropylene (PP) is one of the commonest thermoplastics known. Since it is a thermoplastic, PP has properties as above in section 2.2.2 classification of polymers but is much lighter, stiffer, and more resistant to sunlight when compared to other thermoplastics like PP. Some of its uses include making tubing, firm, bottles, cups, electrical insulation, packaging etc.

Its chemical structure (composition) is as shown below.

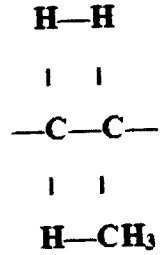

Partly crystalline

(Ashby and Jones, 1995)

2.3 Introduction to Sisal

Sisal is obtained from the leaves of the plant agave sisalana and is now mainly cultivated in East Africa, Brazil, Haiti, India and Indonesia (Nilsson, 1975: Mattoso et al, 1997). It is grouped under the broad heading of the "hard fibres" among which sisal is placed second to manila in durability and strength (Wending, 1947). And yields a stiff fibre used in making rope. (The term may refer either to the plant or the fibre, depending on context) It is not really a variety of hemp, but named so because hemp was for centuries a major source for fibre, so other fibres were sometimes named after it. Sisals are sterile hybrids of uncertain origin; although shipped from the port of Sisal in Yucatan (thus the name); they do not actually grow in Yucatan. (Nilsson). Evidence of an indigenous cottage industry in Chiapas suggests it as the original location, possibly as a cross of Agave Angustifolia and Agave Kewensis.

Sisal is considered a plant of the tropics and subtropics, since production benefits from temperatures above 25 degrees Celsius and sunshine. The sisal plant has a 7-10 year life-span and typically produces 200-250 commercially usable leaves. Each leaf contains an average of around 1000 fibres. The fibre element, which accounts for only about 4% of the plant by weight, is extracted from the leaf either by retting, by

contains an average of around 1000 fibres. The fibre element, which accounts for only about 4% of the plant by weight, is extracted from the leaf either by retting, by scraping or by retting followed by scraping or by mechanical means using decorticators by a process known as decortication (KVIC, 1980). The diameter of the fibre varied from 100μm to 300μm (Mukherjee & Satyanaravana). In the process of decortication, leaves are crushed and beaten by a rotating wheel set with blunt knives, so that only fibres remain. All other parts of the leaf are washed away by water. Decorticated fibres are washed before drying in the sun or by hot air. Proper drying is important as fibre quality depends largely on moisture content. Artificial drying has been found to result in generally better grades of fibre than sun drying. Dry fibres are machine combed and sorted into various grades, largely on the basis of the previous in-field separation of leaves into size groups.

Sisal farming initially caused great environmental degradation, because sisal plantations replaced native forests, but is still considered less damaging than most. No pesticides or chemical fertilizers are used in sisal production, and although herbicides are occasionally used, even this impact may be eliminated, since most weeding is done by hand. (www.advancedbuilding.org)

In East Africa, the leaves are transported to a central decortication plant after which the fibre is dried, brushed and baled for export. In Brazil it is mainly grown by smallholders and the fibre is extracted by teams using portable raspadors. Superior quality sisal is found in East Africa, once washed and decorticated.
Sisal plants consist of a rosette of sword-shaped leaves about 1.5 to 2 meters tall. Young leaves may have a few minute teeth along their margins, but lose them as they mature.

Figure 2.3.1 Picture of Sisal plant and Sisal fibres

(a) Sisal Plant

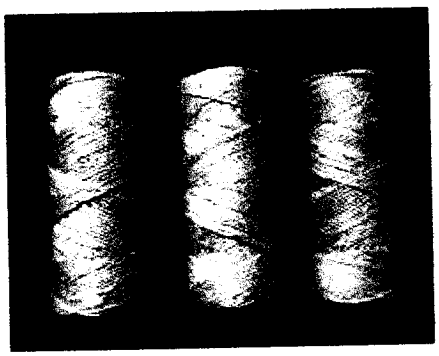

(b)

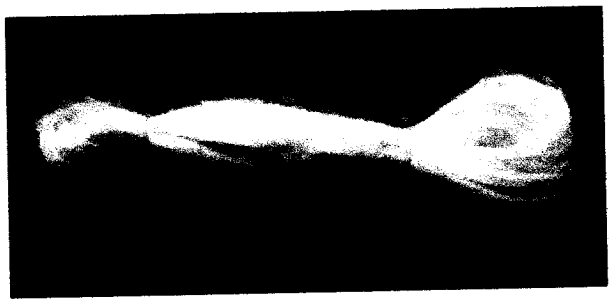

(c)

(b) & (c) Sisal fibres

In the 19th century, Sisal cultivation was spread worldwide, from Florida to the Caribbean islands and Brazil, as well as to countries in Africa, notably Tanzania and Kenya, and Asia. Among flax, hemp, abaca and other agro-based fibre species, annual sisal production is the second largest worldwide, after cotton.

Thousands of tons of sisal fibres are produced annually. In 2003 Tanzania produced approximately 22,000 tons, Kenya produced 22,000 tons and 8,000 tons were produced in Madagascar. China contributed 40,000 tons with smaller amounts coming from South Africa, Mozambique, Haiti, Venezuela and Cuba. In Mexico production has fallen from 160,000 tons in the 1960's to about 15,000 tons today. The first commercial plantings in Brazil were not made until the late 1930's and the first sisal fibre exports from there were made in 1948. It was not until the 1960's that Brazilian production really accelerated and the first of many spinning mills were established. Today Brazil is the major world producer of sisal at 125,000 tons. Sisal occupies 6th place among fibre plants, representing 2% of the world's production of plant fibres (plant fibres provide 65% of the world's fibres).

Sisal fibres are typed by properties relational to the performance of the fibre. Researcher Sara Kadolph found that sisal fibres are smooth, straight and yellow and can be long or short. Since sisal is fairly coarse and inflexible, Kadolph found that sisal can be used by itself or in blends with wool and acrylic for a softer hand. Sisal is valued for cordage use because of its strength, durability, ability to stretch, affinity for certain dyestuffs, and resistance to deterioration in saltwater. Sisal is used by industry in three grades. The lower grade fibre is processed by the paper industry because of its

high content of cellulose and hemicelluloses. The medium grade fibre is used in the cordage industry for making: ropes, baler and binders twine. Ropes and twines are widely employed for marine, agricultural, and general industrial use. The higher-grade fibre after treatment is converted into yarns and used by the carpet industry.

Products made from sisal are being developed rapidly, such as furniture and wall tiles made of resinated sisal. Other products developed from sisal fibre include carpets spa products, cat scratching posts, lumbar support belts, rugs, slippers, cloths and disc buffers. Sisal wall covering meets the abrasion and tearing resistance standards of the American Society for Testing and Materials and of the National Fire Protection Association. Traditionally, sisal has been the leading material for agricultural twine ("binder" and "baler" twine) but the importance of this is diminishing with competition from polypropylene and other techniques evolving. Apart from ropes, twines and general cordage sisal is used in low-cost and specialty paper, dartboards, buffing cloth, filters, geo-textiles, mattresses, carpets, handicrafts, wire rope cores and macramé. In recent years sisal has been utilised as a strengthening agent to replace asbestos and fibre glass as well as an environmentally friendly component in the automobile industry. Products made from sisal fibre are purchased throughout the world and for use by the military, universities, churches and hospitals.

Products made with sisal fibre have the following characteristics. Despite the yarn durability sisal is known for, slight matting of carpeting may occur in high traffic areas. Sisal does not build up static nor does it trap dust, so vacuuming is the only maintenance required. High spill areas should be treated with a fibre sealer and for spot removal, a dry cleaning powder is recommended. Depending on climatic conditions, sisal will absorb air humidity or release it causing expansion or contraction thus not recommended for areas that receive wet spills, or rain or snow.
Mukherjee & Satyanaravana (1984) have studied the mechanical properties of sisal fibre such as initial modulus (the extent to which the fibre resists the deformation in the low strain region called the initial modulus of the fibre), ultimate tensile strength, average modulus and percent elongation as a function of fibre diameter, test length and the speed of testing. It was reported that tensile properties of fibre vary with test length of the fibre. Tables 2.3.1 and 2.3.2 list the observed variation of tensile properties with test lengths and speed of testing respectively. From Table 2.3.1 both

tensile strength and percent elongation decrease with test length, whereas, Young's modulus and average modulus increase with test length. In natural fibres, since the flaws or weak links are irregularly spaced in the fibre, the strength will depend on the length of the fibre used for the tensile test (McLaughlin, 1980).

Table 2.3.1 Variation of tensile properties of sisal fibre with test length (diameter of fibre: 200μm). (Mukherjee & Satyanaravana 1984)

Test Length (mm)	Initial Modulus (GNm^{-2})	Tensile Strength ($MN\ m^{-2}$)	Elongation at Break (%)	Average Modulus ($GN\ m^{-2}$)
15	14.15	793.80	8.15	9.74
25	17.26	757.10	5.70	13.28
35	19.71	728.10	4.65	15.64
50	22.52	630.10	3.98	15.83
65	25.36	620.81	3.50	17.87

Source: Kuruvilla Joseph (1999)

Table 2.3.2 Variation of tensile properties of sisal fibre with speed of testing (diameter of fibre: 200μm; test length: 50mm) (Mukherjee & Satyanaravana 1984)

Speed of Testing ($mm\ min^{-1}$)	Initial Modulus ($GN\ m^{-2}$)	Tensile Strength ($MN\ m^{-2}$)
1	8.41	481.00
2	20.00	608.80
10	22.12	630.12
50	34.16	759.70
500	-	441.60

Source: Kuruvilla Joseph (1999)

If a fibre having length L and strength σ is now changed in length by dL a corresponding change in strength $d\sigma$ will be observed. The incremental change can be related by the equation given below:

$$d\sigma = \alpha \frac{dL}{L} \qquad (2.3.1)$$

where, dL represents the probability of having an imperfection introduced or reduced,

L represents the probability of already having an imperfection in L and α represents a measure of the frequency of occurrence of weak links in the fibre. So with an increase in test length, the number of weak links or imperfections increases, thus resulting in reduction in tensile strength and percent elongation values. The stress-strain curve for sisal fibres was characterised by an initial linear region followed by a curvature indicating the viscoelastic nature of the fibre. The applied stress is shared between crystalline and non-crystalline components in a natural fibre, which is also basically a fibre-reinforced composite on a microscale. As the applied stress increases, the weak primary cell wall collapses and decohesion of cells begins following decohesion of cellulosic and non-cellulosic molecules mainly through weak links and imperfections. This leads to the curvature of the stress-strain curve. The applied stress also causes the uncoiling as well as extensions of the crystalline fibrils in the secondary walls of the cells.

Padmavathi & Naidu (1998) have studied the chemical resistance and tensile strength of sisal fibres (*Agave Veracruz*). It was noted that sisal fibres were more resistant to concentrated HCl compared to other acids. The fibres treated with 18% solution of NaOH showed more tensile load than the other chemically modified fibres. Edwards et al, (1997) have studied the application of FT-Raman microscopy to the non-destructive analysis of sisal fibres. Chand & Joshi (1995) have investigated the effect of gamma irradiation on structure and dc conductivity of this sisal fibre. It was found that exposure of sisal fibre to gamma-irradiation increased the dc conductivity, which has been explained on the basis of microstructure. Singh et al. (1998) have studied the adsorptive interaction between sisal fibre and coupling agents using contact angle measurements and Fourier transform infrared spectroscopy. It was found that high contact angle and reduced hydroxyl groups on titanate-treated fibres favor its better hydrophobicity over the other treatments. The presence of adsorbed layer of coupling agent on the fibre surface was ascertained by appearance, shifting, and decreased intensity of absorption bands. The lowest polar component of surface-free energy for N-substituted methacrylamide-treated fibre indicates the formation of ordered layers of its organofunctionality at the surface. The reason for enhanced interaction between sisal fibre and N-substituted ethacrylamide is suggested by the formation of hydrogen bond, besides extracting a surface-active proton from the fibre surface by alkoxy group to form a covalent bond. An optimum treating condition of fibre for effective

adsorptive interaction has been reported. The deposition of compound in the form of an aggregate on the fibre surface was also observed under scanning electron microscopy.

TABLE 2.3.4 WORLD SISAL PRODUCTION

Top ten sisal and other agave fibres producers — 2006 (thousand metric tonne)	
Brazil	247.6
Tanzania	27.8
Mexico	26.6
Kenya	25.0
Colombia	21.4
China	20.0
Madagascar	17.0
Cuba	11.7
Haiti	5.5
Nicaragua	4.4
World Total	**427.8**
Source: UN Food & Agriculture Organisation (FAO)	

Source: Wikipedia, the free encyclopedia

2.4 Introduction to Kenaf

Kenaf is a 4,000 year old crop with roots in ancient Africa. A member of the hibiscus family (Hibiscus Cannabinus L.), it is related to the family of cotton and okra, and grows well in many parts of the United States. Kenaf grows quickly, rising to heights of 3.5 – 4.5 meters (12 to 14 feet) in as little as 4 to 5 months. The stalks consist of two kinds of fibre: an outer fibre (bast) and an inner fibre (core). The bast is comparable to softwood tree fibres, while the core is comparable to hardwood fibres. After harvest, the plant is processed to separate these fibres for various products. The U.S. Department of Agriculture studies show that Kenaf annually yields of 6 to 10 tons of dry fibre per acre, which is generally 3 to 5 times greater than the yield for Southern pine trees. Kenaf is generally planted in May and harvested in March after drying in the field during the winter months. At the end of the growing season, the kenaf plant flowers. After blooming the flower drops off, leaving a seed pod behind. Kenaf grows well in most parts of the United States and requires few or no pesticides depending on where it is grown. Due to its fibrous stalk insects rarely cause damage. Few chemicals are needed to grow kenaf, but to ensure good soil conditions, some fertilizer and a single herbicide treatment may be used to control weeds. Although kenaf is adaptable to various soils, it grows best in well-drained, sandy loam soil. Kenaf has a relatively wide range of adaptation to climate and soils. With the exception of some early types developed for the Asiatic regions of the former USSR, most of the current kenaf varieties and technologies favor growing at low elevations between 37° N and S latitudes. Optimum growth is generally found in areas like the lower Rio Grande Valley of South Texas with its long, warm growing season and moderate rainfall backed up by irrigation. The kenaf plant is made up of 2 components. The outer periphery is made up of long fibres called the Bast fibres and it occupies around 30 – 40% of the plant by weight. The inner woody component is known as the Core and it weighs around 60 – 70% of the plant. The harvested kenaf plants comprises of the whole stalk (Core and Bast) together. They are bound together by lignin. To separate these 2 components a process called retting is done. (Preston Sullivan, 2003)

There are basically 3 types of retting,

a) Bacterial Retting b) Chemical Retting c) Mechanical Retting

2.4 Introduction to Kenaf

Kenaf is a 4,000 year old crop with roots in ancient Africa. A member of the hibiscus family (Hibiscus Cannabinus L.), it is related to the family of cotton and okra, and grows well in many parts of the United States. Kenaf grows quickly, rising to heights of 3.5 – 4.5 meters (12 to 14 feet) in as little as 4 to 5 months. The stalks consist of two kinds of fibre: an outer fibre (bast) and an inner fibre (core). The bast is comparable to softwood tree fibres, while the core is comparable to hardwood fibres. After harvest, the plant is processed to separate these fibres for various products. The U.S. Department of Agriculture studies show that Kenaf annually yields of 6 to 10 tons of dry fibre per acre, which is generally 3 to 5 times greater than the yield for Southern pine trees. Kenaf is generally planted in May and harvested in March after drying in the field during the winter months. At the end of the growing season, the kenaf plant flowers. After blooming the flower drops off, leaving a seed pod behind. Kenaf grows well in most parts of the United States and requires few or no pesticides depending on where it is grown. Due to its fibrous stalk insects rarely cause damage. Few chemicals are needed to grow kenaf, but to ensure good soil conditions, some fertilizer and a single herbicide treatment may be used to control weeds. Although kenaf is adaptable to various soils, it grows best in well-drained, sandy loam soil. Kenaf has a relatively wide range of adaptation to climate and soils. With the exception of some early types developed for the Asiatic regions of the former USSR, most of the current kenaf varieties and technologies favor growing at low elevations between 37° N and S latitudes. Optimum growth is generally found in areas like the lower Rio Grande Valley of South Texas with its long, warm growing season and moderate rainfall backed up by irrigation. The kenaf plant is made up of 2 components. The outer periphery is made up of long fibres called the Bast fibres and it occupies around 30 – 40% of the plant by weight. The inner woody component is known as the Core and it weighs around 60 – 70% of the plant. The harvested kenaf plants comprises of the whole stalk (Core and Bast) together. They are bound together by lignin. To separate these 2 components a process called retting is done. (Preston Sullivan, 2003)

There are basically 3 types of retting,

a) Bacterial Retting b) Chemical Retting c) Mechanical Retting

In Bacterial retting the whole stalk kenaf plant is immersed in water at room temperature for a period of 5 to 22 days. During this period, due to bacterial action in the whole stalk, the lignin gets dissolved and the bast fibres are separated from the core. Chemical retting is a process done to achieve the separation of bast and core rapidly.In this process the whole stalk kenaf is placed in an alkali bath for a period of one or two hours. The alkali dissolves all the lignin and separates out the fibres from the core. The fibres are washed after the process and are immediately neutralised. The chemical retting changes certain properties in the fiber and the core due to the chemical action on the fibres. There is a loss in tenacity, lusture and color. It also gives low strength and elongation when compared to the fibres that are obtained by bacterial retting.

Mechanical retting is a process to separate the core and the bast fibres by mechanical action. This type of retting is very cheap and gives a very high yield as there are no chemicals involved and there is no loss in strength as well. The disadvantage of this process is that the bast fibres remain stiff and brittle and are very difficult to process especially in textile machinery where the fibres are required to be flexible. The stalks are left in the field to allow bacterial or fungal action to take place that loosens the bast from the stalk. This stalk with loose bast fibres on it is subjected to beating process that separates the fibres into two separate parts, the bast and the core. Mechanical retting is practiced in places where bacterial retting cannot be done due to the lack of resources like a pond or a water bath to soak the stalks in water for a period of 20 days. Once the bast fibres are separated from the core they are used for different applications as they have different properties.

The bast fibre is like a conventional textile fiber obtained in bundles and can be cut into a specific length. These fibres are coarse and brittle in nature and are made soft and flexible by adding alkali in water emulsions. The density of the bast fiber is 1.293 + 0.006gm/cm3. (Preston Sullivan, 2003)

Figure 2.4.1 below shows a Kenaf plantation

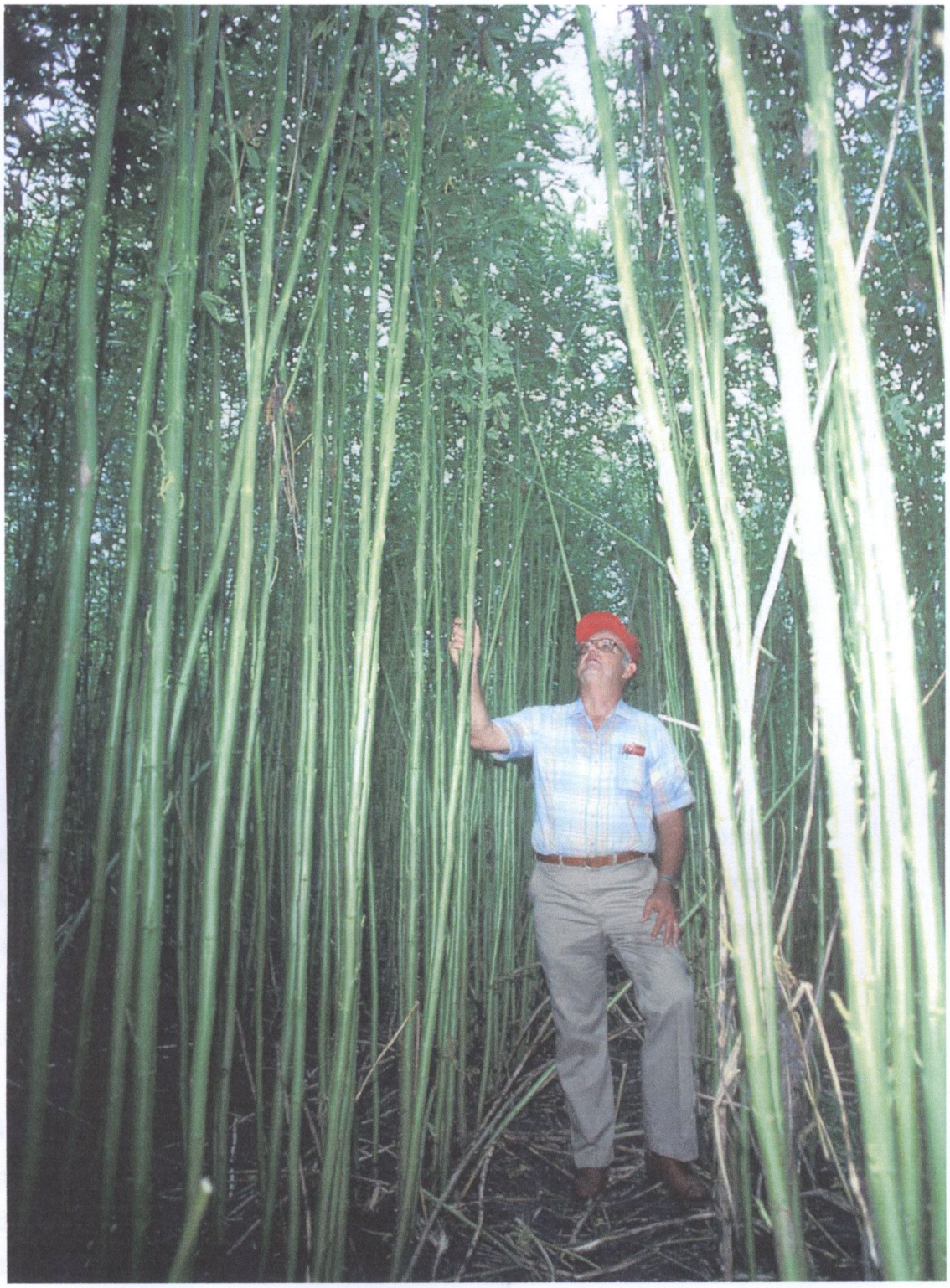

Figure 2.4.1 Kenaf plantation_ (Source Preston Sullivan's report)

Figure 2.4.2 below shows a Kenaf Plant in fields, the cross-section of a kenaf stack and separated bast and core.

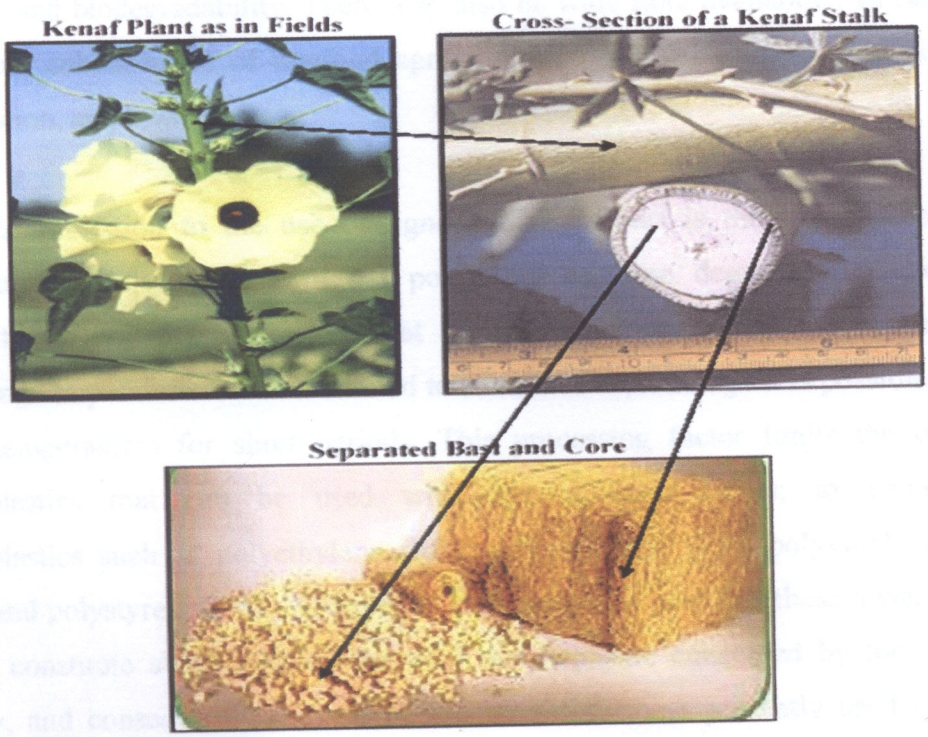

Figure 2.4.2 Kenaf Plant

2.5 Sisal and Kenaf Reinforced Polymers

Since prices for plastics have risen sharply over the past few years. One of the new areas of development is combining natural fibres with thermoplastics thus providing a cost reduction to the plastic industry (and in some cases increases performance as well). Research has concentrated in two basic areas: one in which no attempt is made to compatibilise the two dissimilar resources and, a second in which a compatibiliser is used to make the hydrophore (plastic) mix better with the hydrophil (lignocellulosic). In the first case, the lignocellulosic-fiber is added as relatively low-cost filler and in the second, the lignocellulosic-fiber is added as reinforcing filler. Both of these types of materials are usually referred to as natural fibre /thermoplastic blends. (Rowell et al 1986)

The primary advantages of using lignocellulosic fibres as fillers/reinforcements in plastics are numerous. Such fibres may exhibit low densities, non abrasiveness, high

specific properties (such as high filling levels possibly resulting in high stiffness properties), easily recycled non-brittle fibres, sharp curvature allowances (with no fracture), and biodegradability. There may also be wide fibre availability of rural job generation, enhancement of nonfood agricultural/farm-based economy, low energy consumption, and lower costs.

The main limitation to the use of lignocellulosic fibres is the lower processing temperature permissible due to the possibility of fibre degradation and/or the possibility of volatile emissions that could affect composite properties. The processing temperatures are thus limited to about 200°C, although it is possible to use higher temperatures for short periods. This processing factor limits the type of thermoplastics that can be used with lignocellulosic fibres; to commodity thermoplastics such as polyethylene (PE), polypropylene (PP), polyvinyl chloride (PVC) and polystyrene (PS). However, it is important to note that these lower-priced plastics constitute about 70% of the total thermoplastic consumed by the plastics industry, and consequently the use of fillers/reinforcement presently used in these plastics far outweigh the use in other more expensive plastics.

Another drawback is the high moisture absorption of lignocellulosic fibres. Moisture absorption can result in swelling of the fibre resulting in dimensional stability problems in the lignocellulosic fibre composites. The absorption of moisture by the fibre is minimized in the composite due to encapsulation by the polymer and good fibre-matrix bonding. Good adhesion decreases the rate and amount of water absorbed in the interphase region of the composite. It is difficult to entirely eliminate the absorption of moisture without using expensive surface barriers on the composite surface. The moisture pick up of the fibres can be dramatically reduced. However, moisture absorption can have some secondary benefits, such as reducing static electricity in the final plastic object. (Rowell et al 1986)

Combining Kenaf or Sisal fibre with other resources provides a strategy for producing advanced composite materials that take advantage of the properties of both types of resources. It allows the Engineers to design materials based on end-use requirements within a framework of cost, availability, recyclability, energy use, and environmental considerations. Kenaf and Sisal fibre are potentially outstanding reinforcing filler in

thermoplastic composites. The specific tensile and flexural moduli, for example, of a 50% by volume of kenaf-PP composite compares favorably with a 40% by weight of glass fibre-PP injection molded composite. Results indicate that Kenaf fibres are a viable alternative to inorganic/mineral-based reinforcing fibres as long as the right processing conditions and aids are used, and for applications where the higher water absorption of the lignocellulosic-based fibre composite is not critical. (Rowell et al 1986)

Table 2.5.1 Comparison data between Glass and Kenaf reinforced Polypropylene

Filler Reinforcement in PP	Unit	None	Kenaf	Glass
Filler by Weight	--	0	50	40
Filler by Volume	--	0	39	19
Tensile strength	MPa	33	65	110
Specific Tensile Modulus	MPa	33	61	89
Flexural strength	MPa	41	98	131
Specific Flexural strength	MPa	46	92	100
Flexural Modulus	GPa	1.4	33	6.2
Specific Flexural Modulus	MPa	1.6	6.8	5
Elongation at Break	--	10	2.2	2.5
Notched Izod Impact	Jm	24	32	10

Comparison data taken form modern plastic encyclopedia (1993) and machine design: Material selector issue (1994)

2.6 Fatigue in Natural Fibre Reinforced Polymers (NFRP)

The failure of a material under the action of repeated fluctuating or cyclic load, namely fatigue, after a certain number of cycles has been recognised as one of the major causes of failure in metals. This stress level is often much lower than that required to cause fracture under static loading.

Three basic factors are necessary to cause fatigue. These are:

- Maximum tensile stress of sufficiently high value
- Large enough variation or fluctuation in the applied stores, and
- Sufficiently large number of cycles of the applied stress.

In addition, there are a host of other variables, such as stress concentration, corrosion, temperature, overload, residual stresses and combined stresses which tend to alter the conditions for fatigue

For metals the fatigue process is generally understood, being attributed to stable crack propagation from existing crack-like defects or crack initiation and propagation from structure micro-flaws know as dislocations. The cyclic action of load causes the crack to grow until it is so large that the remainder of the cross-section cannot support the load. At this stage there is a catastrophic propagation of the crack across the material in a single cycle. If the NFRP article has not been properly moulded, introduction of flaws capable of crack propagation is a possibility, and the initiation phase of failure will be negligible. If the article has been moulded this tends to produce a protective skin layer which inhabits fatigue crack initiation or propagation. In such cases it is more probable that that fatigue cracks will develop from within the bulk of the material. In this case the initiation of cracks capable of propagation may occur through slip of molecules if the polymer is crystalline. In amorphous polymers it is possible that cracks may develop in the voids which are formed during viscous flow. In common with other materials the fatigue processes in NFRP are dominated by randomly occurring events so that it is not uncommon to find a lot of scatter in the test results. Fatigue failures are always brittle and are particularly serious because there is no visual warning that failure is imminent. The knowledge of dislocation theory for metals is at an advanced stage. In this case the completely different molecular structure means that there is unlikely to be a similar type of crack initiation process although it is possible that once a crack has been initiated, the propagation phase may be similar. (George E. Dieter, 1988)

Typical forms of cyclic loading that occur in real structural materials are almost random in nature and vary in magnitude during their service life. Five characteristics in constant amplitude cyclic loading where the amplitude and mean stress stay constant are cyclic stress amplitude, σ_a, mean stress ,σ_m, maximum stress ,σ_{max}, minimum stress ,σ_{min}, and the stress ratio, R. any two of the above quantities are sufficient to complete define the cyclic loading. The mean or steady state stress σ_m is the average algebraic sum of the maximum, σ_{max} and minimum, σ_{min} cyclic stresses. The alternating or variable stress amplitude, σ_a is defined as

$$\sigma_a = \frac{D\sigma}{2} = \left(\frac{\sigma_{max} - \sigma_{min}}{2} \right) \qquad (2.6.1)$$

The stress ratio R is defined as the algebraic ratio of minimum to maximum cyclic stress, i.e.

$$R = \frac{\sigma_{min}}{\sigma_{max}} \tag{2.6.2}$$

Another less commonly used parameter is amplitude parameter, which is expressed as

$$A = \frac{\sigma_a}{\sigma_m} = \left(\frac{1-R}{1+R}\right) \tag{2.6.3}$$

R is widely used to distinguish different constant amplitude cyclic loading conditions in fatigue analysis. Figure 2.6.1 shows the different loadings of fatigue.

2.6.1 Fatigue mechanism

Cracks grow in the way shown in figure 2.6.2. In a pure metal or polymer the tensile stress produces a plastic zone which makes the crack tip stretch open by the amount δ, creating new surface there. As the stress is removed the crack closes and the new surface folds forward, extending the crack (roughly by δ). On the next cycle the same thing happens again, and the crack inches forward, roughly at $da/dN \approx \delta$. Not that the crack can not grow when the stress is comprehensive because the crack faces come into contact and carry the load (crack closure).

Figure 2.6.1.1 below shows different fatigue loading types

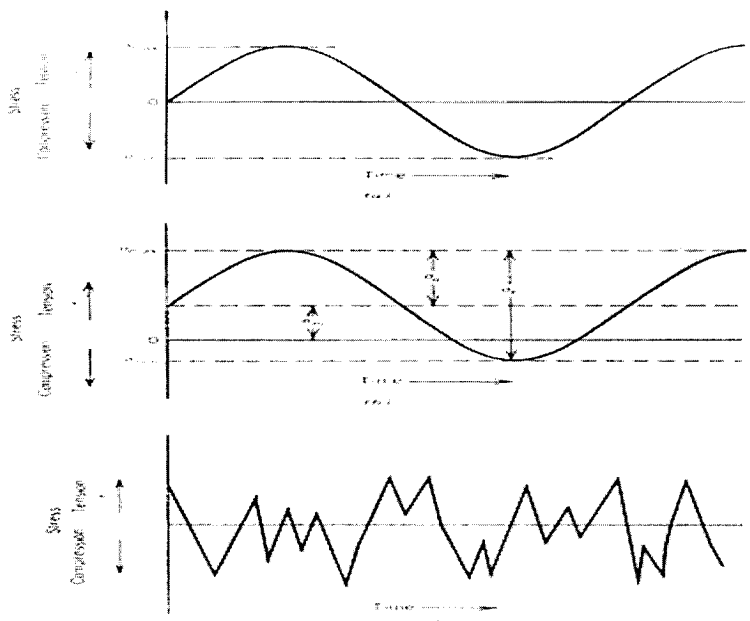

Figure 2.6.1.1 Different fatigue loading types. (*Source*: William, 2005)

Figure 2.6.1 (a) illustrates a completely reversed cycle of stress of sinusoidal form. For this type of stress cycle the maximum and minimum stresses are equal. Tensile stress is considered positive, and compressive stress is negative.

Figure 2.6.1 (b) illustrates a repeated stress cycle in which the maximum stress σ_{max} (Rmax) and minimum stress σ_{min} (Rmin) are not equal. In this illustration they are both tension, but a repeated stress cycle could just as well contain maximum and minimum stresses of opposite signs or both in compression.

Figure 2.6.1 (c) illustrates a complicated stress cycle which might be encountered in a part such as an aircraft wing which is subjected to periodic unpredictable overloads due to gusts.

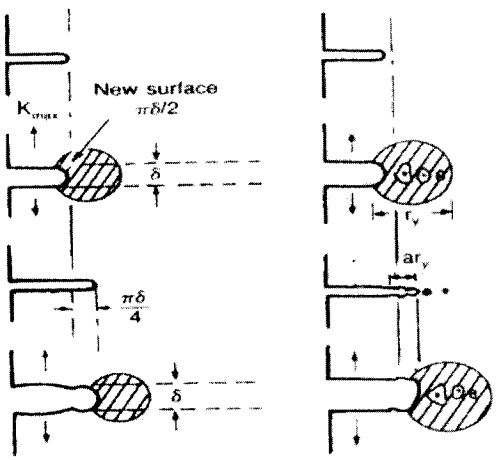

Figure 2.6.2 How fatigue cracks grow. (*Source*: Ashby and Jones, 1996)

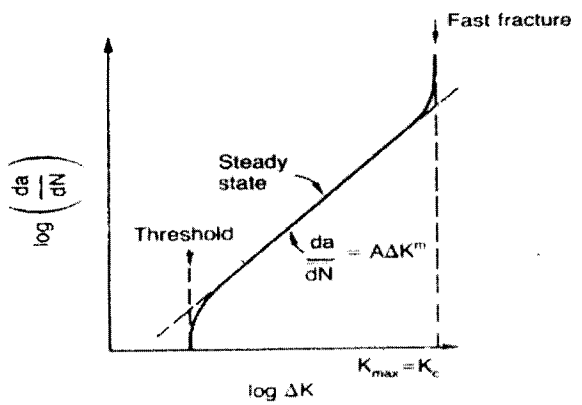

Figure 2.6.3 Crack growth mechanism. (*Source*: Ashby and Jones, 1996)

This records the crack growth rate da/dN (in mm/cycle) as a function of the stress intensity range ΔK. This is relevant to a situation where a crack already exists in the material. The threshold stress intensity range (ΔK_{th}) is the value of ΔK below which no crack growth occurs. This is as shown in figure 2.6.2.

The position of the curve varies with the mean K in the cycle (normally defined in terms of the stress ratio $R = K_{min}/K_{max}$), and other factors.

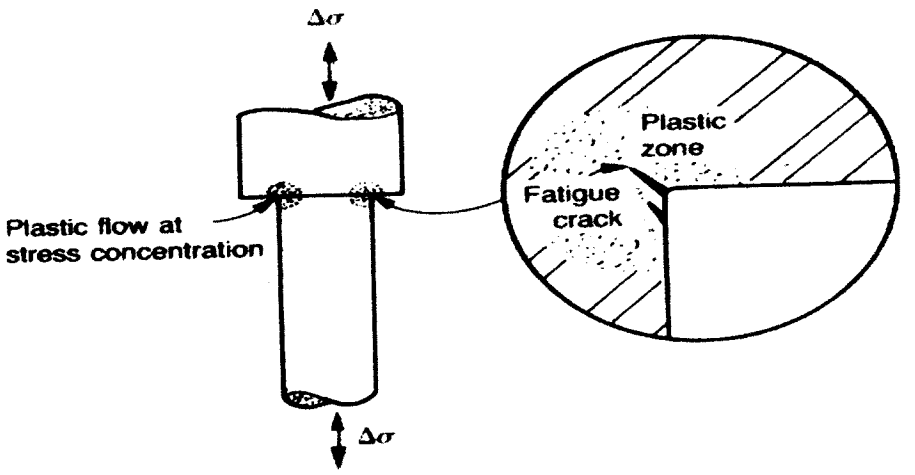

Figure 2.6.4 How cracks form in high-cycle fatigue. (*Source*: Ashby and Jones, 1996)

Fatigue damage is represented by fatigue mechanisms, which nominally occur at ambient or low temperatures. The fatigue life term, N_f^{fat}, is represented by the strain-life relation.

$$\frac{\Delta\varepsilon_m}{2} = C\left[2N_f^{fat}\right]^d \qquad (2.6.4)$$

Where $\Delta\varepsilon_m$ is the mechanical strain range, and C and d is is material constants determined from low-temperature isothermal tests. Figure 2.7 below shows how cracks grow. (Ashby and Jones, 1996)

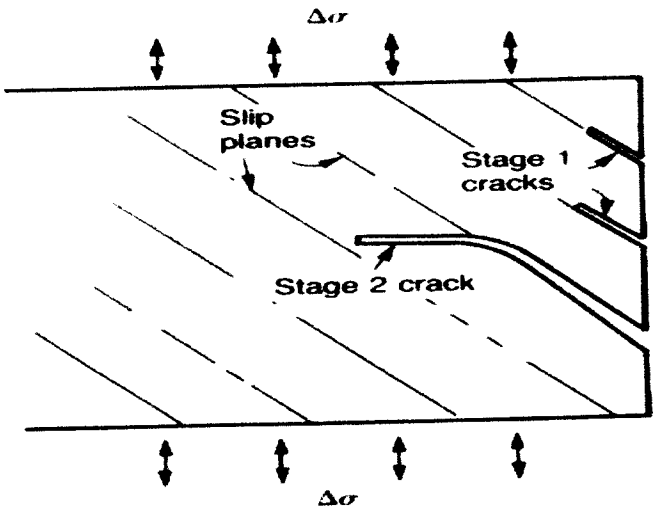

Figure 2.6.5 How cracks grow in low-cycle fatigue. (Source: Ashby and Jones 1996)

2.6.2 Fatigue in Plastic

Although plastics are susceptible to a wider range of failure mechanisms it is likely that fatigue still has an important part to play. Fatigue failures are always brittle and are particularly serious because there is no visual warning that failure is imminent. In the case of polymers where a complete different molecular structure is from metals, means that there is unlikely to be a similar type of crack initiation process although it is possible that once a crack has been initiated, the subsequent propagation phase may be similar.

There are a number of additional features which make polymer fatigue a complex subject and not one which lends itself to simple analysis. The very nature of the loading means that stress, strain and time are all varying simultaneous. The viscoelastic behaviour of the material means that strain rate (or frequency) is an important factor. There are also special variables peculiar to this type or testing such as the type of control (whether controlled load or controlled deformation), the level of the mean load or mean deformation and shape of the cyclic waveform. To add to the complexity, the inherent damping and low thermal conductivity of plastics causes a temperature rise during fatigue. This may bring about deterioration in the mechanical properties of the material or cause it to soften so much that it becomes useless in any load bearing application. (www.tms.org)

Figure 2.6.2.1 below shows how plastics behave under fatigue.

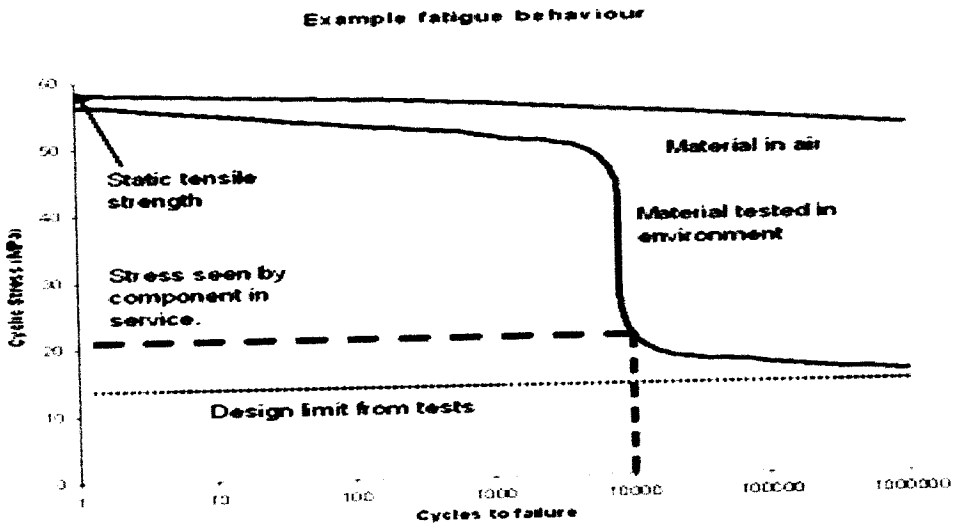

Figure 2.6.2.1 Fatigue behaviour in polymer (*Source*: www.tms.org)

2.6.3 Natural fibre reinforced polymer

For many applications it is possible to increase the modulus and strength of plastics by means of reinforcement. A reinforced plastic consists of two main components; a matrix which may be either thermoplastic or thermosetting and the reinforcing filler which usually takes the form of fibres. In general the matrix has a low strength in comparison to the reinforcement which is also stiffer and brittle. To gain maximum benefit from the reinforcement the fibres should bear as much as possible of the applied stress. The function of the matrix is to support the fibres and transmit the external loading to them by shear at the fibre-matrix interface. Since the fibre and matrix are quite different in structure and properties it is convenient to consider them separately. (Chikampa Sydney, 2008)

2.6.4 Analysis of reinforcement plastics

Theoretical analysis of composite system can be complicated because fibre length, diameter and orientation are all factors. Simple theoretical treatments can be of the mixtures in the relation to the modulus and strength of a reinforced material. The relationship are valid for a composite consisting of continuous fibres uni-axially aligned in a uniform elastic matrix when tested in the direction of the reinforcement. (Chikampa Sydney, 2008)

2.6.6 S-N curve

The basic method of presenting engineering fatigue data is by means of the S-N curve, a plot of stresses S against the number of cycles to failure N. A log scale is almost always used for N. The value of stress that is plotted can be σ_a, σ_{max} or σ_{max} The stress values are usually normal stresses, i.e., there is no adjustment for stress concentration. The S-N relationship is determined for a specific value of σ_m. Most determinations of the fatigue properties of materials have been made in completed reversal bending, where the mean stress is zero. It should be noted that this S-N curve is concerned chiefly with fatigue failure at high number of cycles ($N>10^5$ cycles).

The reason why some materials always have definite fatigue limit has been a subject of many studies and has been determined and this occurs only in alloys in which strain aging takes place. It should be noted however, that no fatigue limit is observed in steels and other alloys normally exhibiting one when they are exposed in a fatigue element in a corrosive environment. (Sonat, *et al*)

Figure 2.6.6.1 below shows the fatigue curve for non-ferrous metals.

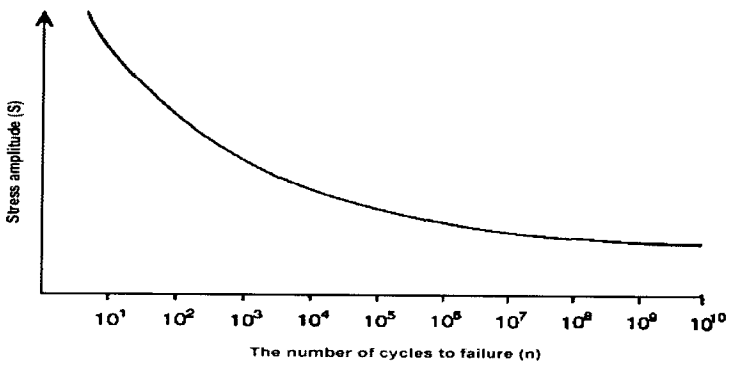

Figure 2.6.6.1 Fatigue curve for non-ferrous metals (source: Sonat, *et al*)

2.6.7 Fatigue life estimation

The effects of fatigue are cumulative and it is difficult to predict the fatigue life of components which work under varying conditions of stress. The assessment of such damage becomes particularly important when one deals with materials in which the fatigue properties are measured by a finite endurance limit. Let certain stress amplitude σ_{ai} is N_{ei}. The fraction of the life used is then N_i/N_{ei}. Let another stress

amplitude σ_{aj} corresponding to N_{ej} on the S-N curve be applied for N_j cycles. An additional fraction of the life N_j/N_{ej} is then used. The PALMGREN-MINER rule states that fatigue failure is expected when such life fractions sum to unity (William, 2005).

Thus $$\frac{N_i}{N_{ei}} + \frac{N_j}{N_{ej}} + \frac{N_k}{N_{ek}} = 1 \qquad (2.6.7.1)$$

Figure 2.6.7.1 shows life prediction for various amplitude loadings which is complete reversed.

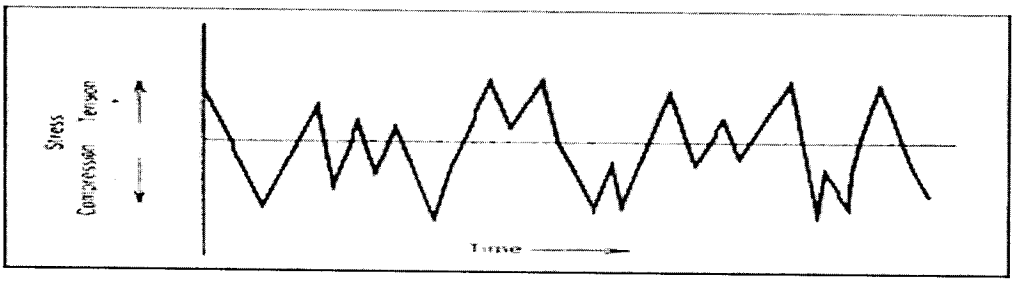

Figure 2.6.7.1 Life prediction for various amplitude loadings which is complete reversed (*Source*: William, 2005)

2.6.8 Statistical nature of fatigue

Since fatigue life and fatigue limit are statistical quantities, it must be realised that considerable deviation from an average curve determined with only a few specimens is to be expected. It is necessary to think in terms of probability of a specimen attaining a certain life at a given stress or the probability of failure at a given stress in the vicinity of the fatigue limit. To do this requires the testing of considerably more specimens than in the past so that the statistical parameters for estimating these probabilities can be determined.

In determining the fatigue limit of a material, it should be recognised that each specimen has its own fatigue limit, a stores above which it will fail but below which it will not fail, and that this critical stress varies from specimen to specimen for very obscure reasons,

The statistical problem of accurately determining the fatigue limit is complicated by the fact that we can not measure the individual value at the fatigue limit of any given specimen. We can only test a specimen at a particular stress and if the specimen fails, then the stress was somewhere above the fatigue limit of the specimen. (George E. Dieter, 1988)

2.6.9 Effect of mean stress on fatigue

Much of the fatigue data in the literature have been determined for conditions of completely reversed cycles of stress, $\sigma_m = 0$. However, conditions are frequently met in engineering practices where the stress situation consists of an alternating stress and a superimposed mean, or steady, stress. There are several possible methods of determining an S-N diagram for a situation where the mean stress is not equal to zero.

Figure 2.6.9.1 below shows the combination of properties which maximise the stiffness to weight ratio and strength to weight ratio, for various loading geometries

Mode of loading	Optimum stiffness	Optimum strength
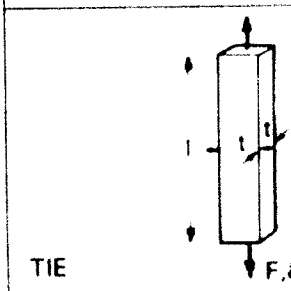 TIE	$\delta = \frac{Fl}{Et^2}$ $M = \rho l t^2$ $= \left(\frac{l^2 F}{\delta}\right)\frac{\rho}{E}$ Maximise $\frac{E}{\rho}$	$\sigma_y = \frac{F}{t^2}$ $M = \rho l t^2$ $= Fl\left(\frac{\rho}{\sigma_y}\right)$ Maximise $\frac{\sigma_y}{\rho}$
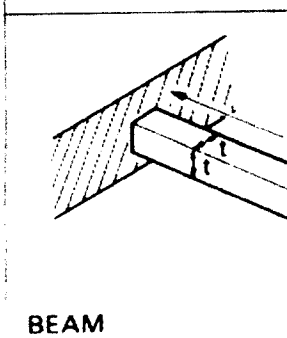 BEAM	$\delta = \frac{4Fl^3}{Et^4}$ $M = \rho l t^2$ $= 2\left(\frac{Fl^5}{\delta}\right)^{1/3}\left(\frac{\rho}{E^{1/3}}\right)$ Maximise $\frac{E^{1/3}}{\rho}$	$\sigma_y = \frac{6Fl}{t^3}$ $M = \rho l t^2$ $= l(6Fl)^{2/3}\left(\frac{\rho}{\sigma_y^{2/3}}\right)$ Maximise $\frac{\sigma_y^{2/3}}{\rho}$
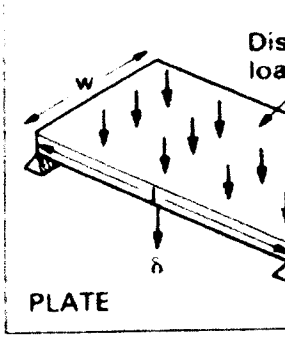 PLATE	$\delta = \frac{5Fl^3}{32Ewt^3}$ $M = \rho l w t$ $= l^2\left(\frac{5Fw^2}{32\delta}\right)^{1/3}\left(\frac{\rho}{E^{1/3}}\right)$ Maximise $\frac{E^{1/3}}{\rho}$	$\sigma_y = \frac{3Fl}{4wt^2}$ $M = \rho l w t$ $= \left(\frac{3Fl^3 w}{4}\right)^{1/2}\left(\frac{\rho}{\sigma_y^{1/2}}\right)$ Maximise $\frac{\sigma_y^{1/2}}{\rho}$

E = Young's modulus; σ_y = Yield strength; ρ = Density

Figure 2.6.8.1 The combination of properties which maximise the stiffness to weight ratio and strength to weight ratio, for various loading geometries. (Source: Ashby and Jones, 1996)

2.7 Design of Composite Materials and Structures

A composite material is defined as a material in which two or more distinct materials are combined together but remain uniquely identifiable in the mixture. The most common example is, perhaps, fibreglass, in which glass fibres are mixed with a polymeric resin. If the composite was cut and after suitable preparation of the surface then look at the material, the fibres and polymer resin would be easy to distinguish. This is not the same as making an alloy by mixing two distinct materials together where the individual components become indistinguishable. An example of an alloy that most people are familiar with is brass, which is made from a mixture of copper and zinc. After making the brass by melting the copper and zinc together and solidifying the resultant mixture, it is impossible to distinguish either between or where the atoms of copper and zinc are. Regardless of the actual composite, the two [or more] constituent materials that make up the composite are always readily distinguished when the material is sectioned or broken.

To design a composite material we must first identify the numerous materials related variables that contribute to the mechanical and physical properties of the composite material. Secondly, the appropriate physical and mathematical models that describe how the properties of the individual components of the composite are combined to produce the properties of the composite material itself must be derived. So it is possible to design a composite material such that it has the attributes desired for a specific application. Those attributes might be as simple has having a specified stiffness and strength, a desired thermal conductivity, or have a minimum specified stiffness at the cheapest possible cost per unit volume. Whatever the specifications it should be possible to design a suitable composite material. As in all design processes, it may not be possible to meet all the specifications exactly and compromise and tradeoffs will be required, but by understanding the physical origin of the required properties and developing an appropriate mathematical description, a suitable composite can be designed. There are also many different ways in which the fibres can be combined into the resin, for example, are the fibres all aligned in the same direction, are the fibres woven into a cloth, what type of cloth, are the fibres aligned at random, and are the fibres long or short? Then, if the fibres are oriented, at what angle relative to the fibres, are the fibres being loaded? Finally, just what is the ratio of fibres to resin is in the composite in terms of the volume ratio or weight ratio?

By looking at the range of fibre products available and by seeking clarification on the structure and composition of the fibre we can identify the micro structural variables that will control the properties of the composite. These may be summarized as

- The properties of the fibre reinforcement.
- The properties of the matrix in which the reinforcement is placed.
- The amount of reinforcement in the matrix.
- The orientation of the reinforcement.
- The size and shape of the reinforcement.

(Zoltan Mezey 1997)

2.7.1 Loading Parallel to Aligned Continuous Fibres.

If the composite material is to stay in equilibrium then the force (F) we apply to the composite as a whole, F must be balanced by an equal and opposite force in the fibre, F_f and the matrix F_m.

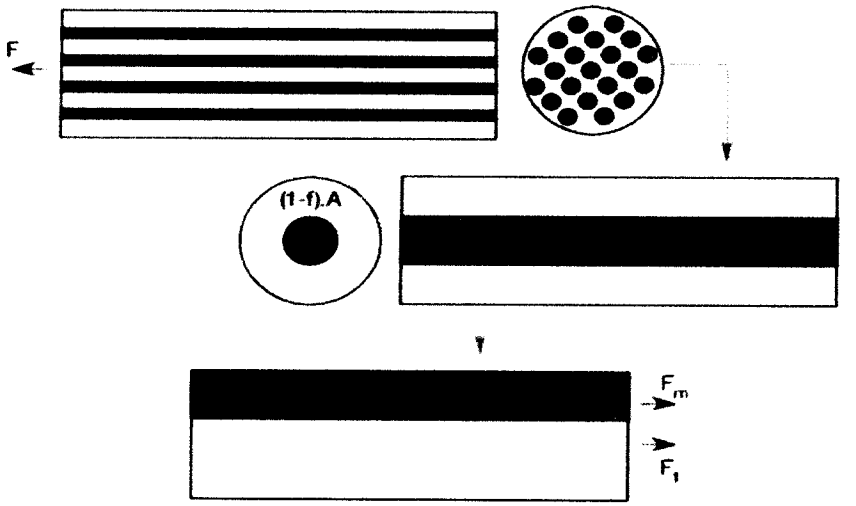

Figure 2.7.1.1 Shows a composite loaded parallel to aligned continuous fibres.

The force on the fibres is equal to the stress in the fibres multiplied by the cross sectional area of the composite occupied by the fibres, f i.e. the volume fraction of the fibres multiplied by the cross-sectional area of the composite itself, f.A. Similarly the force on the matrix is just the stress in the matrix multiplied the cross-sectional area of the matrix in the composite, i.e. (1-f).A. So the stress in the composite is just the sum

of the stresses in the fibres and the matrix multiplied by their relative cross-sectional areas as the Area of the composite is constant.

$$F = F_f + F_m$$
$$\sigma \cdot A = \sigma_f \cdot fA + \sigma_m \cdot (1-f)A$$
$$\sigma = \sigma_f \cdot f + \sigma_m \cdot (1-f) \qquad (2.7.1.1)$$

The stress in the fibre and the stress in the matrix are generally not the same so Hooke's Law is used. This applies as long as the stresses are below the elastic limit and the material in question is linear elastic which is true for many polymers.

$$\sigma = E\varepsilon,$$

where E is the elastic modulus.

For compatibility, the strain must be the same in both the fibres and the matrix otherwise holes would appear in the ends of the composite as we stretched it. This is known as the ISOSTRAIN rule.

$$\varepsilon \cdot E = \varepsilon_f \cdot E_f \cdot f + \varepsilon_m \cdot E_m \cdot (1-f)$$
$$\varepsilon \cdot E = \varepsilon \cdot E_f \cdot f + \varepsilon \cdot E_m \cdot (1-f)$$
$$E = E_f \cdot f + E_m \cdot (1-f) \qquad (2.7.1.2)$$

Since the fibre and matrix often have quite different elastic moduli then the stress in each must be different in fact the stress is higher in the material with the higher elastic modulus (usually the fibre). For example in fibreglass, the elastic modulus of the glass (~75GPa) is much greater than that of the polyester matrix (~5GPa) so as the volume fraction of fibres is increased, the elastic modulus of the composite (measured parallel to the fibres) increases linearly with the volume fraction of fibres. (Zoltan Mezey 1997)

2.7.2 Loading Perpendicular to Aligned Continuous Fibres

If the load is applied perpendicular to the fibre axis then the composite would respond in a very different way.

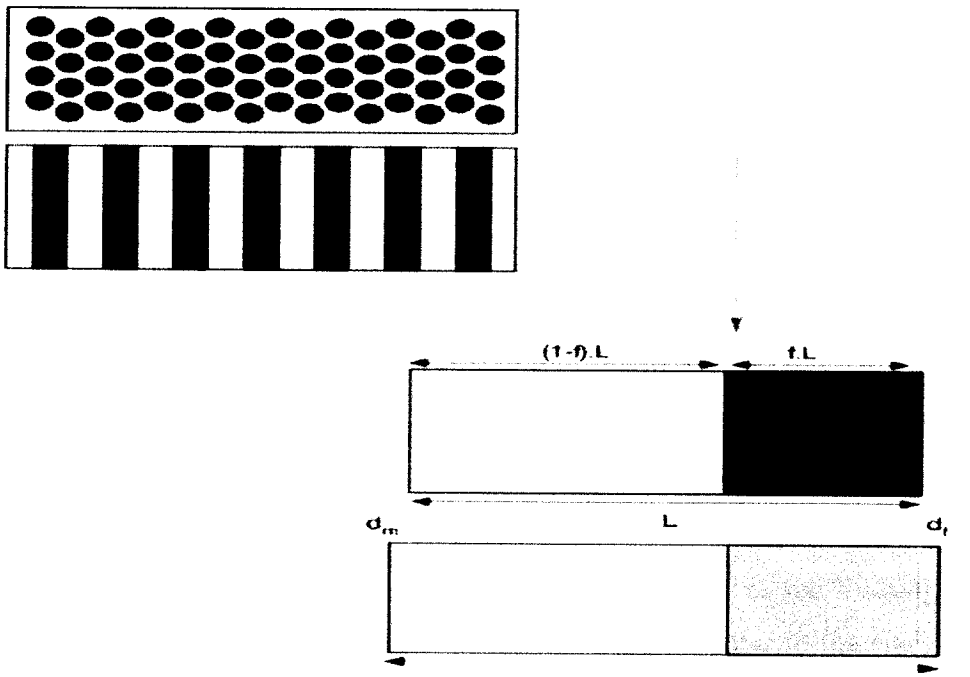

Figure 2.7.2.1 Shows a composite loaded perpendicular to aligned continuous fibres

In a fibrous composite with the applied stress aligned perpendicular to the fibres, the stress is transferred to the fibres through the fibre matrix interface and both the fibre and the matrix experience the same stress If the matrix and fibre have different elastic properties then each will experience a different strain and the strain in the composite will be the volume average of the strain in each material. Since the stress is the same in each phase this is known as the ISOSTRESS rule of mixtures. If a force is applied perpendicular to the fibres then the fibres and matrix will stretch in the same direction. The total deflection (d) is just the sum of the deflections in the fibre (d_f) and the matrix (d_m).

$$d = d_f + d_m$$
$$\varepsilon \cdot L = \varepsilon_f \cdot fL + \varepsilon_m \cdot (1-f)L$$
$$\varepsilon = \varepsilon_f \cdot f + \varepsilon_m \cdot (1-f) \qquad (2.7.2.1)$$

Since deflection is just strain multiplied by the initial length, substituting for the deflections results in elimination of L as it appears in every term of the resulting equation. Again, Hooke's law introduces the elastic modulus and since the stress is the same in both the matrix and fibre, elastic modulus perpendicular to the fibres can be obtained. (Zoltan Mezey 1997)

$$\frac{\sigma}{E} = \frac{\sigma_f}{E_f} \cdot f + \frac{\sigma_m}{E_m} \cdot (1-f)$$

$$\frac{\sigma}{E} = \frac{\sigma}{E_f} \cdot f + \frac{\sigma}{E_m} \cdot (1-f)$$

$$\frac{1}{E} = \frac{1}{E_f} \cdot f + \frac{1}{E_m} \cdot (1-f)$$

$$E = \frac{E_m \cdot E_f}{f \cdot E_m + (1-f) \cdot E_f} \qquad (2.7.2.2)$$

The stiffness of the composite, measured perpendicular to the fibres increases much more slowly than stiffness measured parallel to the fibres as the volume fraction of fibres is increased. Since the properties of the composite are different in different directions, the composite is anisotropic. In both instances the limiting values of the stiffness of the composite, either parallel or perpendicular to the fibres are given by the elastic moduli of the fibre and matrix materials. It is however important to note that in the derivations above we have assumed that both the matrix and fibre are elastically isotropic and thus the fibres have the same elastic modulus when stretched parallel to the fibre axis and when loaded in a radial direction. This is certainly the case for this project, sisal and kenaf, but it is not the case when composites containing organic fibres such as graphite, kevlar, pbo etc., are manufactured. Due to the highly aligned and linear nature of the organic molecules making up the fibre, the elastic modulus of the fibre in the radial direction is often 10 to 20 times lower than in the axial direction because in the axial direction stiffness arises primarily from the resistance to rotation and stretching of the C-C bonds that make up the molecular structure of the fibre while in the transverse or radial direction it is the relatively weak intermolecular Van der Waals bonds that are being stretched.

i.e.

$$E = \frac{E_m \cdot E_{f_t}}{f \cdot E_m + (1-f) \cdot E_{f_t}} \qquad (2.7.2.3)$$

where E_{ft} is the transverse elastic modulus of the fibre.

In a real composite, there is actually a limit to the amount of the reinforcement that can be added to the matrix in order that the matrix can transfer the load to the reinforcing material. (Zoltan Mezey 1997)

2.7.3 Fibre Packing

The equations which predict the properties of a composite breakdown at high volume fractions of reinforcement because of geometric packing limitations and the necessity for the reinforcing phase to be surrounded by the matrix in order that load can be transferred to it. There are two simple packing models which can be used to establish an upper bound for the volume fraction, a square array and a hexagonal array with circular section reinforcement.

2.7.3.1 Hexagonal close packing

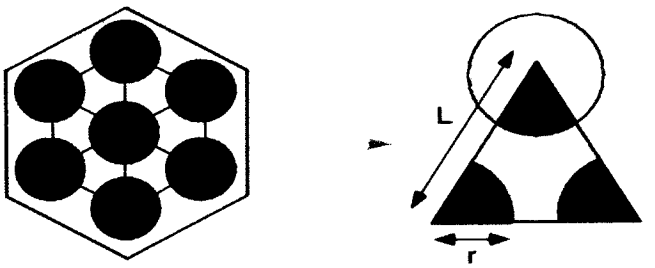

Figure 2.7.3.1.1 Shows a Hexagonal close packing in composites.

$$f = \frac{Area\ of\ Fibre}{Area\ of\ Matrix}$$

$$f = \frac{3 \cdot \frac{\pi r^2}{6}}{\frac{1}{2}L \cdot L\sin\left(\frac{\pi}{3}\right)} = \frac{2\pi r^2}{\sqrt{3}L^2} \qquad (2.7.3.1.1)$$

The maximum volume fraction of fibres, f_{max} occurs when the fibres are just touching, i.e.

$$L = 2r \qquad (2.7.3.1.2)$$

So,

$$f_{max} = \frac{\pi}{2\sqrt{3}} = 0.907 \qquad (2.7.3.1.3)$$

2.7.3.2 The simple cubic packing

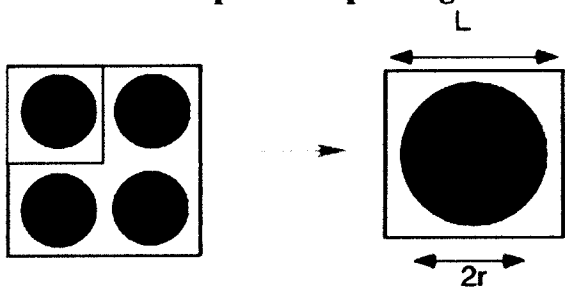

Figure 2.7.3.2.1 Shows a simple cubic packing.

$$f = \frac{Area\ of\ Fibre}{Area\ of\ Matrix}$$

$$f = \frac{\pi r^2}{L^2} \qquad (2.7.3.2.1)$$

The maximum volume fraction of fibres occurs when the fibres are just touching, i.e. $L = 2r$

So,

$$f_{max} = \frac{\pi}{4} = 0.786 \qquad (2.7.3.2.2)$$

From the two figures it is readily apparent that volume fractions higher than 90% are impossible and that even 78% fibre loading would be very difficult to achieve. In practice, the maximum volume fraction is around 60% in unidirectional aligned fibre composites. In woven materials, the total volume fraction rarely exceeds 40% in a given layer of cloth and so the effective fibre fraction in either the warp or weft directions is unlikely to exceed 20% for a plain weave fabric. For loosely packed fabrics such as chopped strand mat, the total volume fraction of fibres is unlikely to exceed 10% and is normally used to provide filler layers between the outer load bearing layers in a multilayer laminate. (Zoltan Mezey 1997)

2.7.4 Density, Weight and Volume

The density of the composite is easily calculated by adding up the mass of each component

$$M = M_f + M_m$$
$$M = \rho \cdot V$$
$$\rho \cdot V = \rho_f \cdot V_f + \rho_m \cdot V_m$$
$$\rho \cdot V = \rho_f \cdot f \cdot V + \rho_m \cdot (1 - f) \cdot V$$
$$\rho = f\rho_f + (1 - f)\rho_m \qquad (2.7.4.1)$$

Converting volume fraction of fibres, f, to weight fraction of fibres, f_w and weight fraction, f_w, to volume fraction, f, is achieved by the two formulae below respectively.

$$f = \frac{V_f}{V_f + V_m}$$

$$f = \frac{\frac{M_f}{\rho_f}}{\frac{M_f}{\rho_f} + \frac{M_m}{\rho_m}}$$

$$f = \frac{\frac{f_w M}{\rho_f}}{\frac{f_w M}{\rho_f} + \frac{(1-f_w)M}{\rho_m}}$$

$$f = \frac{f_w}{f_w + (1-f_w)\frac{\rho_f}{\rho_m}} \qquad (2.7.4.3)$$

$$f_w = \frac{M_f}{M_f + M_m}$$

$$f_w = \frac{\rho_f \cdot fV}{\rho_f \cdot fV + \rho_m \cdot (1-f)V}$$

$$f_w = \frac{f\rho_f}{f\rho_f + (1-f)\rho_m} \qquad (2.7.4.2)$$ and

2.7.5 Elastic-Brittle, Matrix Fails First

The first case considered is that where both the fibre and the matrix are linear elastic to failure but the matrix fails at a lower strain than that of the fibre. Strain is the important factor in determining the failure strength of the composite when testing parallel to the fibres because both the fibre and the matrix experience the same strain.

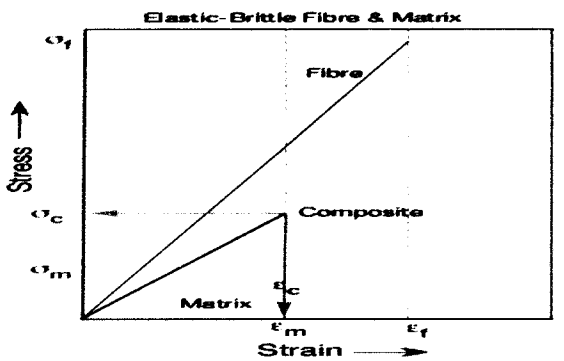

Figure 2.7.5.1 shows a stress-strain curve for an Elastic-Brittle composite were the matrix fails first.

When the strain in the composite reaches the fracture strain of the matrix, the matrix will fail. Immediately before the matrix breaks, the stress being carried by the composite is

$$\sigma = \varepsilon E$$

$$\sigma_c = \varepsilon_c E = \left(fE_f + (1-f)E_m\right)\varepsilon_m \qquad (2.7.5.1)$$

What actually happens to the composite as the matrix breaks depends on how the composite is being loaded and how much fibre is present in the composite. There are two different, but distinct ways that load is imposed on a material, constant deflection and constant load.

2.7.5.1 Loading under constant deflection

In a conventional tensile test the material being tested is actually stretched, i.e. a slowly increasing displacement is applied to one end of the material, the other end remains fixed in place. What is measured is the resistance that the material is imposing against being stretched. If part of the material breaks, like the matrix in the composite is just about to do, the deflection at that instant does not change. The fibres are still stretched by the same strain so the stress in the fibres remains as it was just prior to the matrix failing. Hence, the fibres will not break. However, the load will fall as will the stress on the composite as a whole. The stress in the fibres when the matrix breaks is $\varepsilon_m E_f$, the force required to sustain that stress is $\varepsilon_m E_f fA$. The actual stress on the composite is thus

$$\sigma = \frac{F}{A} = \frac{\varepsilon_m E_f fA}{A} = f\varepsilon_m E_f \qquad (2.7.5.1.1)$$

Since the fibres run the whole length of the composite, the fibres continue to resist the imposed deflection and we can continue to stretch the fibres to their failure strain at which point the stress being carried by the composite is

$$\sigma_c = f.\sigma_f \qquad (2.7.5.1.2)$$

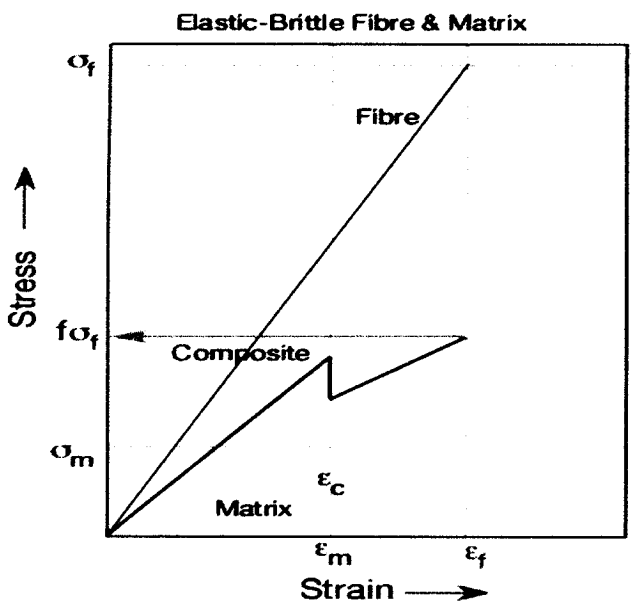

Figure 2.7.5.1.1 Shows the stress-strain curve of an Elastic-Brittle composite loaded under constant deflection.

If $f\sigma_f < (fE_f + (1-f)E_m)\varepsilon_m$ then clearly the ultimate tensile strength of the composite is $(fE_f + (1-f)E_m)\varepsilon_m$ otherwise it's $f\sigma_f$. (Zoltan Mezey 1997)

2.7.5.2 Loading under constant load

In the real world, and cases where materials are tested by imposing slowly increasing loads, what happens when the matrix breaks differs from the case of constant deflection loading. The fibres that remain when the matrix cracks now instantantly have to support the imposed load making the stress in the fibres increase to a higher value because the fibres only occupy a fraction of the original cross-sectional area. Because the stress in the fibres increases, the strain in the fibres also increases and the material will exhibit an increase in deflection (strain) with no additional increase in load. If the increased stress is higher than the failure strength of the fibres then the fibres will break, if not we can continue to increase the load until the fibres break. The stress on the composite at this point is still $f\sigma_f$, as before.

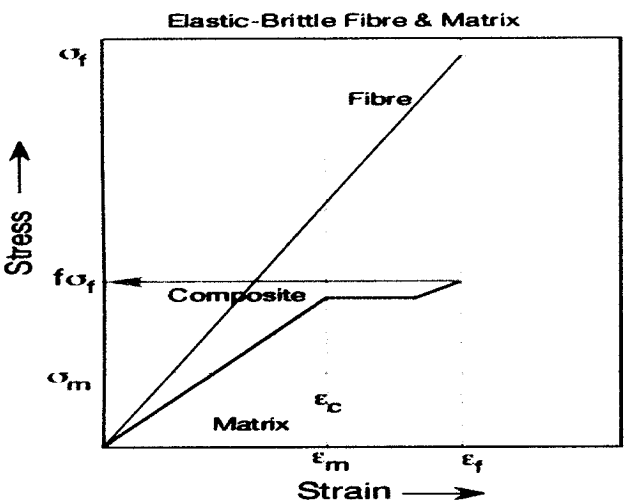

Figure 2.7.5.2.1 Shows the stress-strain curve of a composite loaded under constant load.

In the graph below we plot both equations together with the larger of the two as a function of the volume fraction of fibres.

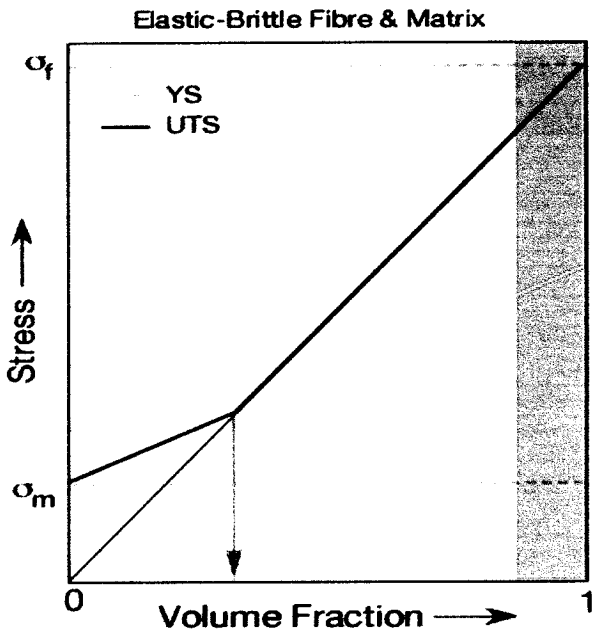

Figure 2.7.5.2.2 Shows a stress-stain curve of a composite as a function of volume fraction of the fibres.

It can be seen that when the volume fraction of fibres is lower, the composite breaks when the matrix fails but when the fibre fraction is above a critical value the composite can remain intact to higher stresses than those required to break the matrix. The concept of "working strength" is important in composites because if the material is unloaded after the matrix has failed, but the fibres remain intact, it can be reloaded. However, the elastic modulus on retesting will not be the same because the matrix takes no part in resisting the applied loads so the modulus just scales as $f.E_f$ which is less than before. The composite could be described as damaged but it is damage tolerant in that even when the matrix has failed it can continue to support an applied load. In real composites the fibres reinforcing the composite are far from perfect and have a range of strengths due to surface imperfections or geometrical (thickness/diameter) variations. Thus the fibres fail at a range of strengths (and strains) and we often observe a progressive onset of failure. (Zoltan Mezey 1997)

The volume fraction of fibres when the composite becomes "Damage tolerant" can be found by equating the two strength equations and solving for f *i.e.*

$$fE_f + (1-f)E_m\varepsilon_m = f.\sigma_f \qquad (2.7.5.1)$$

2.7.6 Elastic-Brittle, Fibres Fail First

When a composite in which the elastic strain to failure of the fibres is less than the strain to failure of the matrix being tested, the fibres will be the first component of the composite to break. The "working strength" of the composite is simply the stiffness of the composite multiplied by the strain to failure of the fibres.

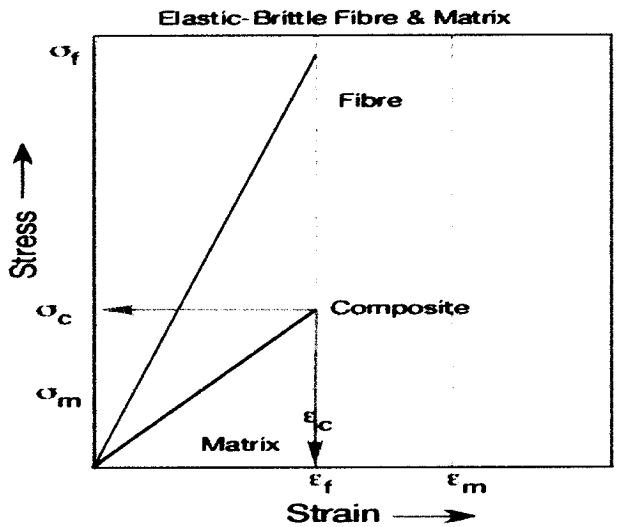

Figure 2.7.6.1 Shows a stress-strain curve for an Elastic-Brittle composite were the fibres fail first.

$\sigma_c = (fE_f + (1-f)E_m).\varepsilon_f$

Again, once the fibres have broken what happens depends on whether the composite is being loaded under conditions of constant deflection or constant load. (Zoltan Mezey 1997)

2.7.6.1 Loading under constant deflection

Once the fibres break, the strain remains the same and since the cross-sectional area of the sample has effectively been reduced by that of the fibres, the load required to maintain that deflection/strain is less than before and the load/stress drops. When the deflection is increased, only the matrix resists and can ultimately be stretched to its failure strain. The stress on the composite is then

$$\sigma_c = (1-f).\sigma_m \qquad (2.7.6.1.1)$$

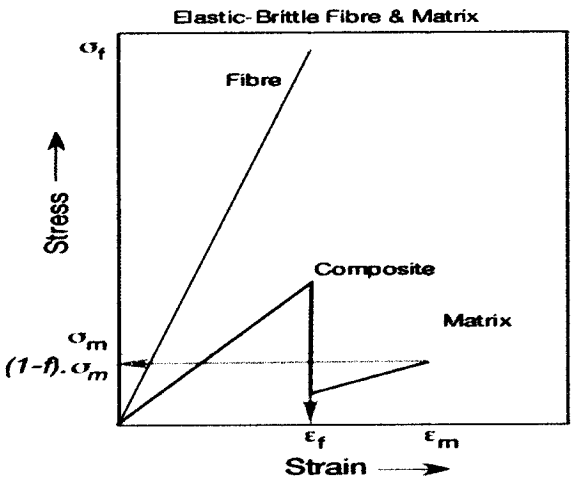

Figure 2.7.6.1.1 Shows a stress-strain curve of a composite loaded under constant deflection.

The ultimate tensile strength of the composite is then the larger of the two stresses.

2.7.6.2 Loading under constant load

When the fibres break, the load is immediately transferred to the matrix, and since the cross sectional area of the matrix is less than that of the composite, the stress in the matrix instantly increases, as does the strain. The increased stress is given by

$$\sigma = \frac{(fE_f + (1-f)E_m).\varepsilon_f}{1-f} \qquad (2.7.6.2.1)$$

Which, if greater than σ_m, will result in fracture of the matrix (and the composite). If the increase in stress is small, such as would be expected at low volume fractions of fibres then the matrix can continue to be loaded until it fails.

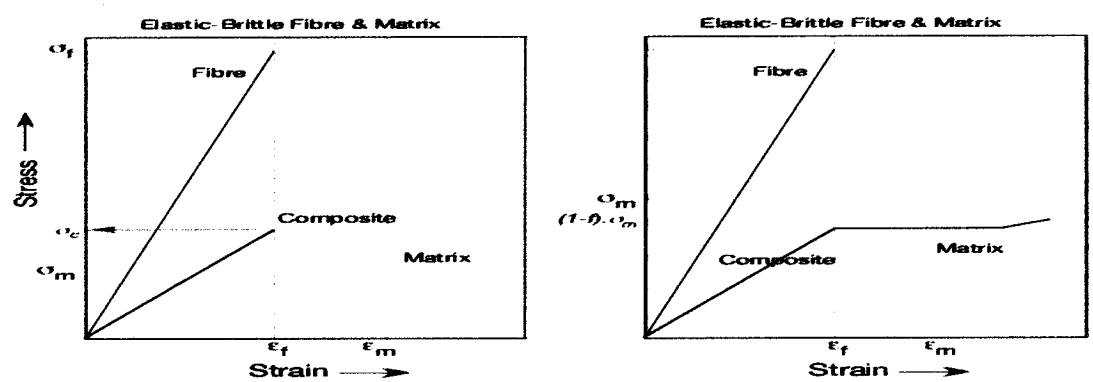

Figure 2.7.6.2.1 Shows a stress-strain curve for a composite loaded under constant load.

Again the final stress being carried by the composite is $\sigma_c = (1-f).\sigma_m$ and like before, the ultimate tensile strength of the composite is the larger of this and the working strength.

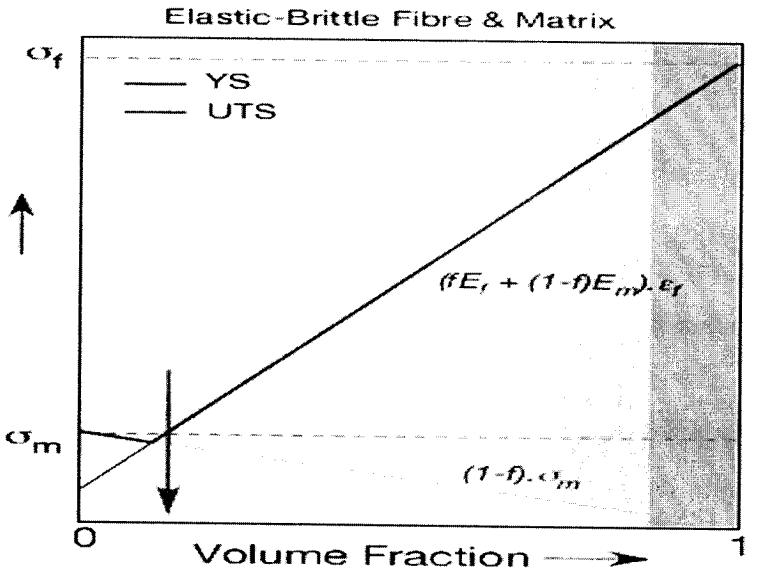

Figure 2.7.6.2.2 Stress-strain curve of a composite for different volume fractions.

Again we can examine the concept of a working strength and an ultimate tensile strength coupled with damage tolerance. When the volume fraction of fibres is low, failure of the fibres does not result in failure of the composite as the matrix alone is capable of supporting the imposed stress. However, just like the case where the matrix failed first, unloading and reloading the composite will result in failure at the reduced matrix strength and the stiffness of the composite will be much reduced. We should also note that when the fibres fail at a lower tensile strain than the matrix, that adding small amounts of fibre produces a composite material with strength less than that of the matrix alone. (Zoltan Mezey 1997)

The volume fraction of fibres when the composite becomes "stronger than the matrix alone" can be found by equating the working strength equation of the composite with the strength of the matrix alone and solving for f *i.e.*

$$\sigma_c = (fE_f + (1-f)E_m).\varepsilon_{f=} \sigma_m \qquad (2.7.6.2.2)$$

CHAPTER THREE

3.0 METHODOLOGY AND WORK DONE.

The project involved simulation of fatigue in NFRP. The simulations were done using computer software Cosmos Works and the physical properties of the reinforced polypropylene were obtained using existing mathematical formulae of volume fraction and but comparison with the experimental results (SILUMWE SYDNEY) was not done because polypropylene was not available to make the specimens. Therefore simulation results from this project were only compared with result from Lyandenga patience (2008) who did fatigue simulation on fibre glass reinforced polyester. Kazuma Plastics Limited in Lusaka's heavy industrial area (a company that specializes in GFRP and makes water tanks and banana boats) was visited to see how the composites are made and also made the specimens of sisal reinforced polyester from the same company. The actual dimensions of the specimen used in the simulations were as shown in figure and the fatigue phenomenon was modeled using cosmos works.

After the modeling, the simulation results were analyzed and, compared with the simulation results of glass-fibre reinforced polymers (Lyandenga P, 2008) and also with the experimental results. Then draw conclusions and made recommendations.

3.1 COMPUTED PHYSICAL PROPERTIES OF THE COMPOSITES

The physical properties of the matrix and the fibres were found from literature by taking the average value of the various sources as shown in the table below.

Table 3.1.1 Table showing the mechanical properties of polypropylene, sisal and kenaf.

.	Polypropylene	Sisal	Kenaf
Tensile Strength (Mpa)	50	550	235
Module, E (Gpa)	1.15	15.6	9.4
Strain, *e* (Gpa)	0.0435	0.0352	0.025

The physical properties of the composites were computed using the volume fraction formulae below:

- First the minimum volume fraction of the fibres in the composite when the strength of the composite is equal to that of the matrix alone was found using the relationships below

  $\sigma_c = (fE_f + (1-f)E_m).\varepsilon_f$

  σ_m

  Simply equating the two strength equations $\sigma_c = (fE_f + (1-f)E_m).\varepsilon_f$ and σ_m then solving for *f*. i.e. $\sigma_c = (fE_f + (1-f)E_m).\varepsilon_f = \sigma_m$

  Sisal:

  $\sigma_c = (fE_f + (1-f)E_m).\varepsilon_f = \sigma_m$

  $[(f \times 15600) + (1-f) \times 1150] \times 0.0352 = 50$, solving for *f* gave

  $\rightarrow f = \underline{0.0187}$

  Kenaf:

  $[(f \times 9400) + (1-f) \times 1150] \times 0.025 = 50$, solving for *f* gave

  $\rightarrow f = 0.1$

  Therefore, the minimum volume fraction of the fibres in the composite when the strength of the composite is equal to that of the matrix alone was found to be 0.0187 and 0.1 for sisal and kenaf fibres respectively.

- The strength of the composite for various volume fractions was obtained using equation (2.7.5.1) and the composite moduli were obtained using the formulae

$$E = \frac{E_m \cdot E_{f_t}}{f \cdot E_m + (1-f) \cdot E_{f_t}}$$ and $$\varepsilon \cdot E = \varepsilon_f \cdot E_f \cdot f + \varepsilon_m \cdot E_m \cdot (1-f)$$ $$\varepsilon \cdot E = \varepsilon \cdot E_f \cdot f + \varepsilon \cdot E_m \cdot (1-f)$$ $$E = E_f \cdot f + E_m \cdot (1-f)$$

depending on the loading of the composite i.e. for ISOSTRESS and ISOSTRAIN loadings respectively. The results were tabulated in a table as shown below. It was these evaluated properties that were inputted into Cosmos Works to determine the static and fatigue phenomenon of NFRP (Sisal and Kenaf) models after running the simulations.

- The density of the composite for the different volume fractions was also obtain using equation 2.7.4.1

Table 3.1.2 Computed mechanical properties of sisal and kenaf composites at different volume fractions.

	Density	**Sisal and polypropylene composite**			**Kenaf and polypropylene composite**		
Volume fraction ,*f.*	Sisal and Kenaf ($Kg/m^{3)}$	Tensile strength (Mpa)	Modulus, E Isostress (Gpa)	Modulus, E Isostrain (Gpa)	Tensile strength (Mpa)	Modulus, E Isostress (Gpa)	Modulus, E Isostrain (Gpa)
0.05	915.5	65.5375	1.206	1.8725	39.0625	1.202	1,5625
0.1	941	90.825	1.267	2.595	49.375	1.261	1.975
0.2	992	141.4	1.411	4.04	70	1.395	2.8
0.3	1043	191.975	1.593	5.485	90.625	1.561	3.625
0.4	1094	242.55	1.827	6.93	111.25	1.772	4.45
0.5	1145	293.125	2.142	8.375	131.875	2.049	5.275
0.6	1196	343.7	2.589	9.82	152.5	2.429	6.1

3.2 RESULTS FROM SIMULATIONS

3.2.1 Sisal reinforced polypropylene

Seven different simulations were done for sisal reinforced polypropylene i.e. for seven different volume fractions. These volume fractions were f=0.05, 0.1, 0.2, 0.3,

0.4, 0.5 and 0.6 but only the results for the volume fraction of f=0.2 are shown in this report.

3.2.1.1 Simulation results for f=0.2

This was done in two stages. First, the model was loaded with a static load of 5000N as shown in the results of the stress and strain plot. The second stage was creating a fatigue study and setting the properties of the study.

The SN curve and the fatigue events were defined after which the simulations were run and results obtained as shown below.

Table 3.2.1.1.1 below shows the physical properties of sisal reinforced polypropylene with a volume fraction f=0.2.

Material name: User Defined

Material Source: Library files

Material Library Name: Sisal reinforced polypropylene f=0.2

Material Model Type: Linear Elastic Isotropic

Property Name	Value	Units	Value Type
Elastic modulus	4.04e+009	N/m^2	Constant
Poisson's ratio	0.4103	NA	Constant
Shear modulus	3.158e+008	N/m^2	Constant
Mass density	992	kg/m^3	Constant
Tensile strength	1.412e+008	N/m^2	Constant
Thermal conductivity	0.147	W/(m.K)	Constant
Specific heat	1881	J/(kg.K)	Constant

Table 3.2.1.1.1 Physical properties of Sisal reinforced polypropylene with f=0.2

Table 3.2.1.1.2 below shows mass and volume of the model used

No.	Part Name	Material	Mass	Volume
1	Sisal reinforced polypropylene.	User Defined	0.0594026 kg	5.98817e-005 m^3

Table 3.2.1.1.3 below shows how and where the restraint and load were applied as well as the magnitude of the load on the model used.

Restraint		
Restraint-1 <Part 2>	on **1 Face(s)** immovable (no translation).	
Load		
Force-1 <Part 2>	on **1 Face** apply force **5000 N** normal to reference plane with respect to selected reference **Face< 1 >** using uniform distribution	Sequential Loading

Table 3.2.1.1.3 Restraint and load applied on the model.

Table 3.2.1.1.4 below shows the mesh and solver information that were applied to the model.

Mesh Information	
Mesh Type:	Solid mesh
Mesher Used:	Standard
Smooth Surface:	On
Jacobian Check:	4 Points
Element Size:	3.9136 mm
Tolerance:	0.19568 mm
Quality:	High
Number of elements:	5702
Number of nodes:	11371

Solver Information	
Quality:	High
Solver Type:	FFE
Option:	Include Thermal Effects
Thermal Option:	Input Temperature
Thermal Option:	Reference Temperature at zero strain: 298 Kelvin

Table 3.2.1.1.4 Mesh and solver information.

Stress results

Table 3.2.1.1.5 Shows the values of the maximum and minimum stresses as well as their location on the model. .

Name	Type	Min	Location	Max	Location
Plot1	VON: von Mises stress	24726 N/m^2 Node: 287	(-206.219 mm, 0 mm, -60 mm)	1.2022e+009 N/m^2 Node: 10800	(-108.559 mm, 1.25 mm, -36 mm)

The maximum stresses are observed to take place around the notch as it is a point of stress concentration. The yield strength is found to be 550Mpa

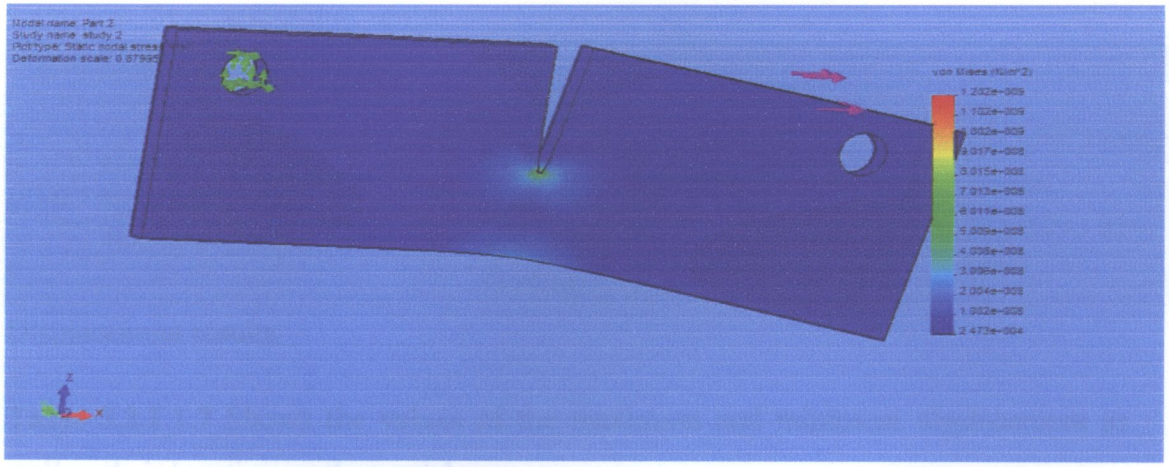

Figure 3.2.1.1.1 Stress results obtained from the simulation.

Strain results

Table 3.2.1.1.6 Shows the values of the maximum and minimum strains as well as their location on the model.

Name	Type	Min	Location	Max	Location
Plot1	ESTRN: Equivalent strain	7.04391e-006 Element: 2739	(-208.603 mm, 0.748508 mm, -59.0625 mm)	0.187084 Element: 2300	(-108.671 mm, 0.625 mm, -36.5625 mm)

The maximum strains are also observed to take place around the notch as it is a point of stress concentration.

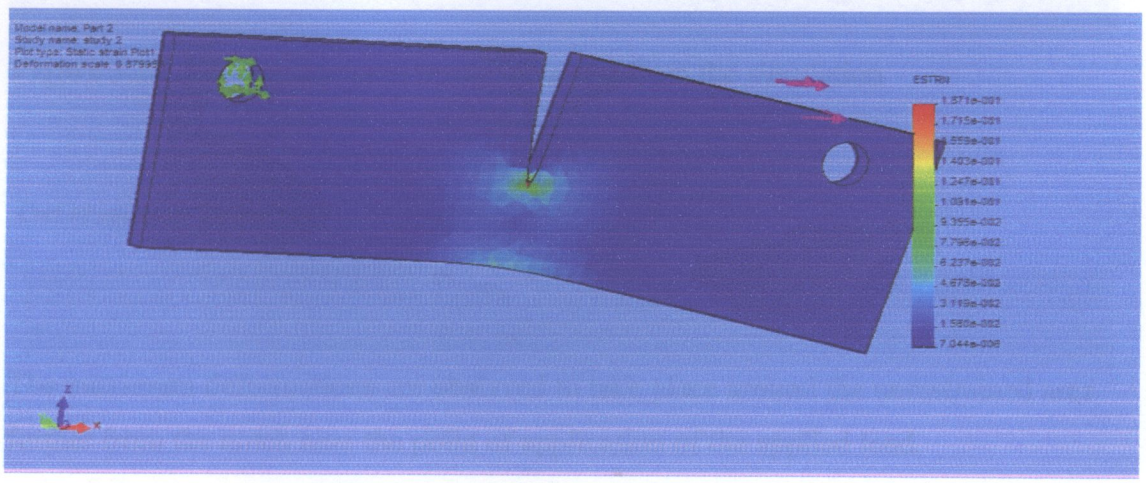

Figure 3.2.1.1.2 Strain results obtained from the simulation

Name	Type	Min	Location	Max	Location
Plot1	URES: Resultant displacement	0 m Node: 19	(-190 mm, 9.63249e-009 mm, -6 mm)	0.02565 m Node: 172	(-6.15095 mm, 0 mm, 1.27609e-014 mm)

Displacement results

Table 3.2.1.1.7 Shows the values of the maximum and minimum displacement as well as their location on the model. .

The maximum displacements are observed to take place around the unrestrained area further from the notch.

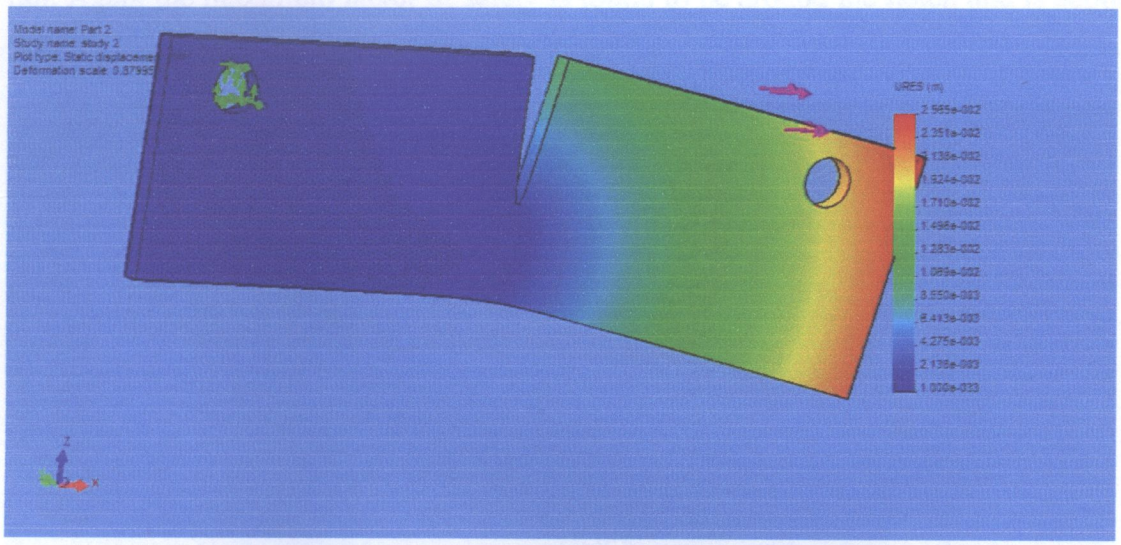

Figure 3.2.1.1.3 Displacement results obtained from the simulation

Deformation Results

Plot No.	Scale Factor
1	0.87995

The maximum deformations are observed to take place around the unrestrained area further from the notch near the point of application of the applied load.

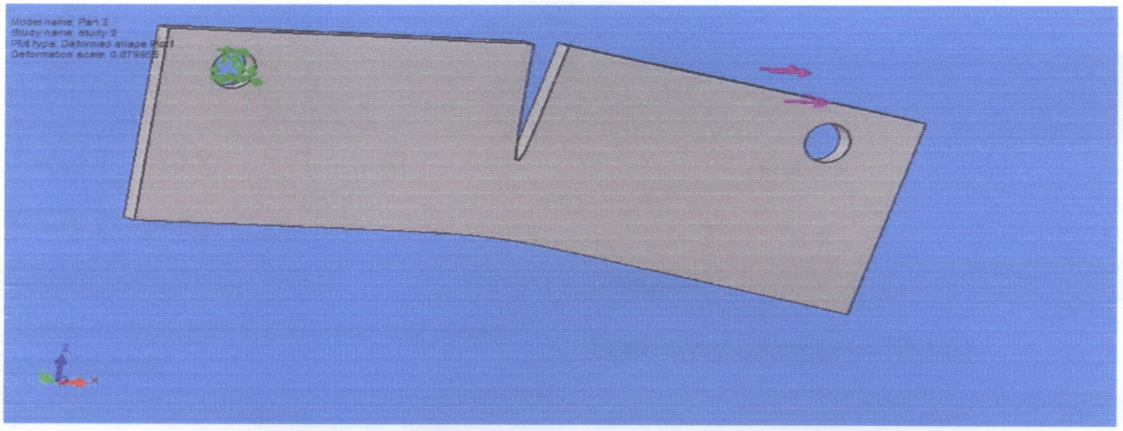

Figure 3.2.1.1.4 Deformation results obtained from the simulation

Design Check Results

The Design check shows the factor of safety distribution in the model if it was not to fail. Again the maximum factor of safety is found to be around the notch and is about 200.

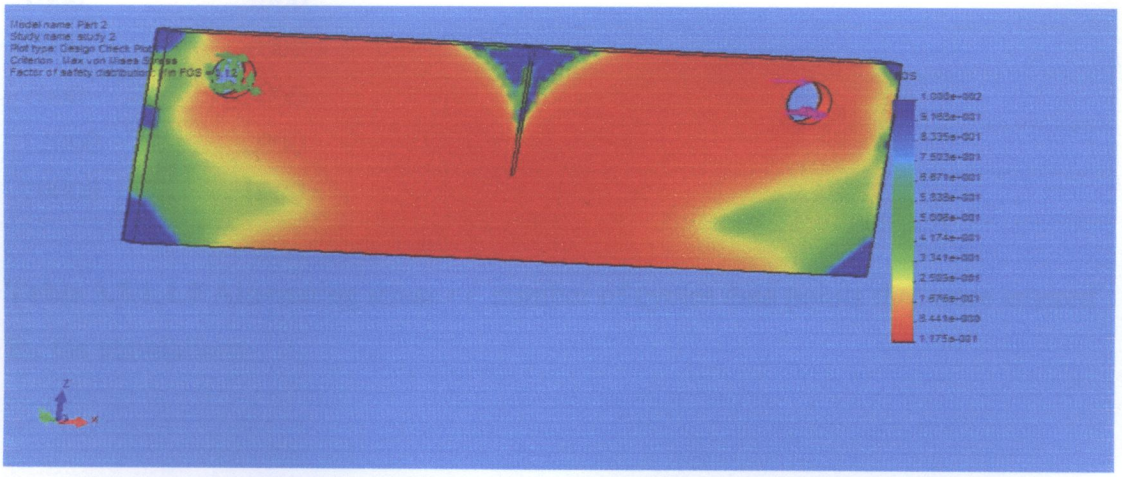

Figure 3.2.1.1.5 Design check results obtained from the simulation

Fatigue analysis.

Table 3.2.1.1.8 Below shows the S-N curve, fatigue loading and some fatigue study properties that were applied to the model. .

S-N Curves

No.	Name	Stress ratio(r)
1	Curve-1	0.200000

Loading

Name	No. of cycles	Loading ratio(LR)	Study(s)
Event-1	1000	0	study 1

Study Property

Interaction between event	Random
Stress component for alternating stress computation	Equivalent stress (von Mises)
S-N curve interpolation	Log-log
Fatigue strength reduction factor(Kf)	0.9

Alternating stress vs. Cycles

Data Points:

Cycles	Alternating Stress (in N/m^2)
1000	5000
3000	4000
7000	3000
12000	2000
20000	1000

Table 3.2.1.1.9 Alternating stress vs. number of cycles data points that were entered for the simulations.

Results

Table 3.2.1.1.10 Shows the values of the maximum and minimum damage, factor of safety, the Biaxiality indicator and the life plot as well as their location on the model.

Name	Type	Min	Location	Max	Location
Plot1	Damage Plot	0.253751 Node: 20906	(-7.69577 mm, 1.25 mm, -58.5 mm)	1 Node: 1	(-30 mm, 9.63249e-009 mm, -6 mm)
Plot2	Factor of Safety Plot	1.72627e-005 Node: 22093	(-108.559 mm, 3.75 mm,	1.37131 Node: 20906	(-7.69577 mm, 1.25 mm,

			-36 mm)		-58.5 mm)
Plot3	Biaxiality indicator plot	-0.999866 Node: 19388	(-205.126 mm, 5 mm, -22.4597 mm)	0.947725 Node: 19843	(-205.432 mm, 2.5 mm, -60 mm)
Plot4	Life Plot	1000 Node: 1	(-30 mm, 9.63249e-009 mm, -6 mm)	3940.88 Node: 20906	(-7.69577 mm, 1.25 mm, -58.5 mm)

Figure 3.2.1.1.6 Below shows the damage plot of the specified fatigue events.

The results for the damage factor indicate that the specified events consume over 100% of the life of the model.

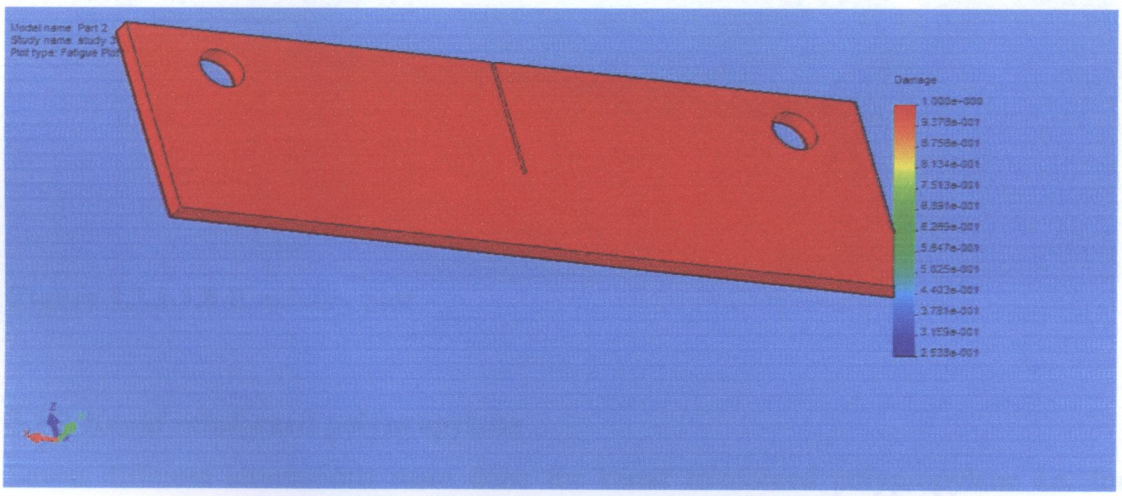

Figure 3.2.1.1.6 Damage plot

Figure 3.2.1.1.7 Below shows the factor of safety plot of the specified fatigue events.

The factor of safety results indicate that the model will fail due to fatigue if the current loads are multiplied by 1.726×10^{-5} (the minimum factor of safety). Since the factor of safety is less than one i.e. (factor of safety<1) our model has already failed. Therefore for our model not to fail we need to multiply the current loads by less than 1.726×10^{-5}.

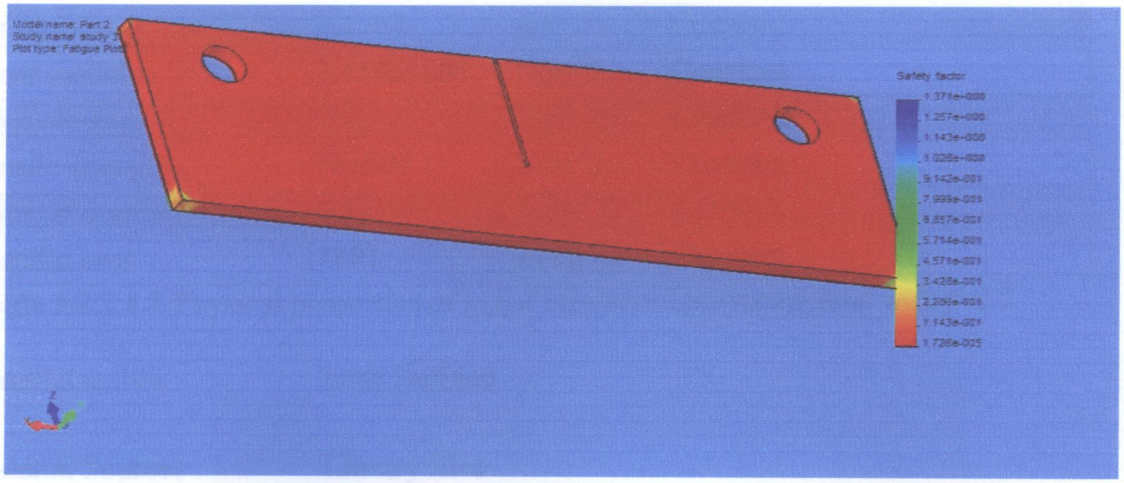

Figure 3.2.1.1.7 Factor of safety plot.

Figure 3.2.1.1.8 Below shows the Biaxiality plot of the specified fatigue events.

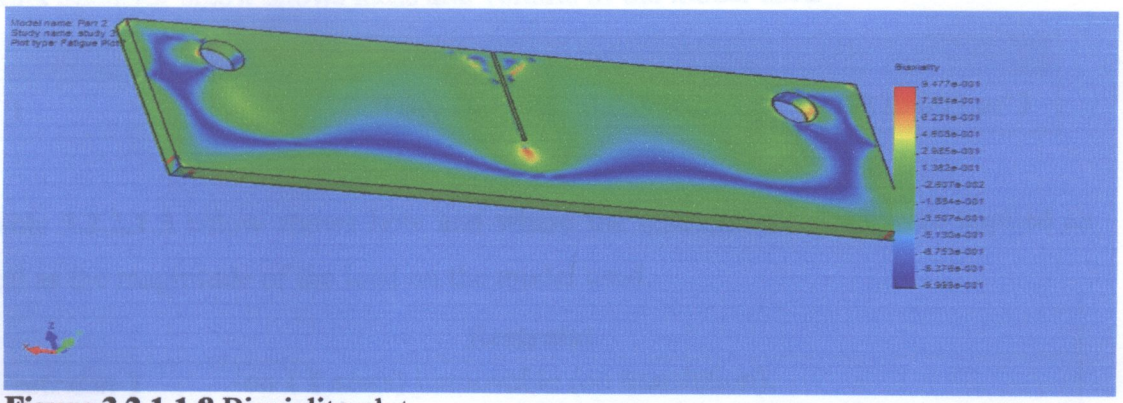

Figure 3.2.1.1.8 Biaxiality plot

3.2.2 Kenaf reinforced polypropylene

Seven different simulations were done for kenaf reinforced polypropylene i.e. for seven different volume fractions. These volume fractions were f=0.05, 0.1, 0.2, 0.3, 0.4, 0.5 and 0.6 but only the results for the volume fraction of f=0.2 are shown in this report.

3.2.2.1 Simulation results for f=0.2

Table 3.2.2.1.1 below shows the physical properties of kenaf reinforced polypropylene with a volume fraction f=0.2.

Property Name	Value	Units	Value Type
Elastic modulus	2.8e+009	N/m^2	Constant

Poisson's ratio	**0.4103**	**NA**	**Constant**
Shear modulus	3.158e+008	N/m^2	Constant
Mass density	**992**	**kg/m^3**	**Constant**
Tensile strength	7e+007	N/m^2	Constant
Thermal conductivity	**0.147**	**W/(m.K)**	**Constant**
Specific heat	1881	J/(kg.K)	Constant

Table 3.2.2.1.1 Physical properties of kenaf reinforced polypropylene with f=0.2

Material name: User Defined

Material Source: Library files

Material Library Name: Kenaf reinforced polypropylene f=0.2

Table 3.2.2.1.2 below shows mass and volume of the model used

No.	Part Name	Material	Mass	Volume
1	Part1	User Defined	**0.0594026 kg**	**5.98817e-005 m^3**

Table 3.2.2.1.3 below shows how and where the restraint and load were applied as well as the magnitude of the load on the model used.

	Restraint	
Restraint-1 <Part1>	on **1 Face(s)** immovable (no translation).	
	Load	
Force-1 <Part1>	on **1 Face(s)** apply force - **1000 N** normal to reference plane with respect to selected reference **Face< 1 >** using uniform distribution	**Sequential Loading**

Table 3.2.2.1.3 Restraint and load applied on the model.

Table 3.2.2.1.4 below shows the mesh and solver information that were applied to the model.

Mesh Information	
Mesh Type:	Solid mesh
Mesher Used:	Standard
Smooth Surface:	On
Jacobian Check:	4 Points
Element Size:	3.9136 mm
Tolerance:	0.19568 mm
Quality:	High
Number of elements:	5702
Number of nodes:	11371

Solver Information	
Quality:	High
Option:	Include Thermal Effects
Thermal Option:	Input Temperature
Thermal Option:	Reference Temperature at zero strain: 298 Kelvin

Table 3.2.2.1.4 Mesh and solver information.

Stress Results

Table 3.2.2.1.5 Shows the values of the maximum and minimum stresses as well as their location on the model.

Name	Type	Min	Location	Max	Location
Plot1	VON: von Mises stress	5611.48 N/m^2 Node: 287	(-206.219 mm, 0 mm, -60 mm)	2.40529e+008 N/m^2 Node: 10800	(-108.559 mm, 1.25 mm, -36 mm)

The maximum stresses are observed to take place around the notch as it is a point of stress concentration. The yield strength is found to be 110Mpa

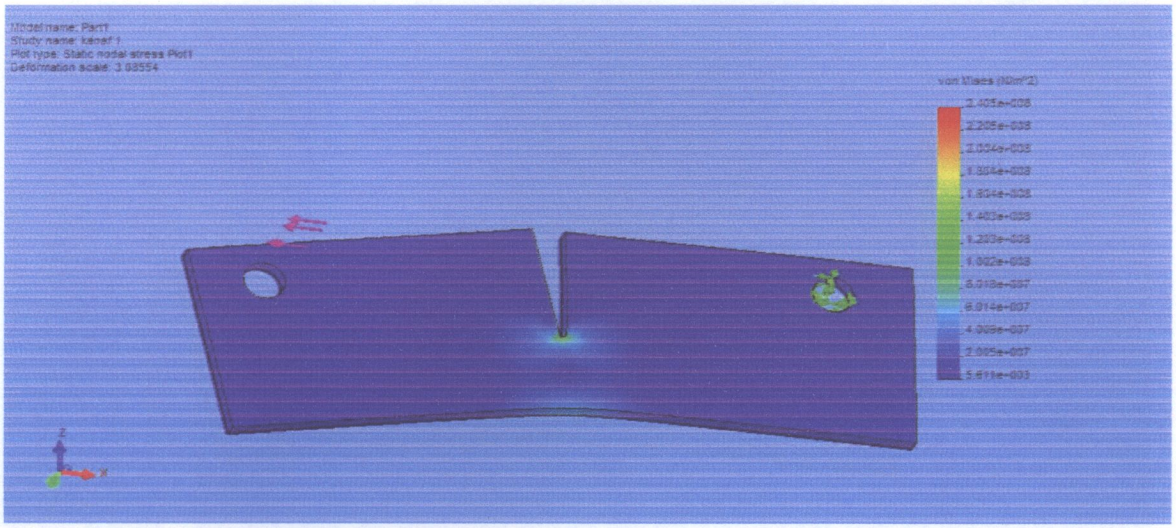

Figure 3.2.2.1.1 Stress results obtained from the simulation

Strain Results

Table 3.2.2.1.6 Shows the values of the maximum and minimum strains as well as their location on the model.

Name	Type	Min	Location	Max	Location
Plot1	ESTRN: Equivalent strain	2.03865e-006 Element: 875	(-7.11281 mm, 4.50282 mm, -58.5653 mm)	0.0540115 Element: 2300	(-108.671 mm, 0.625 mm, -36.5625 mm)

The maximum strains are also observed to take place around the notch as it is a point of stress concentration.

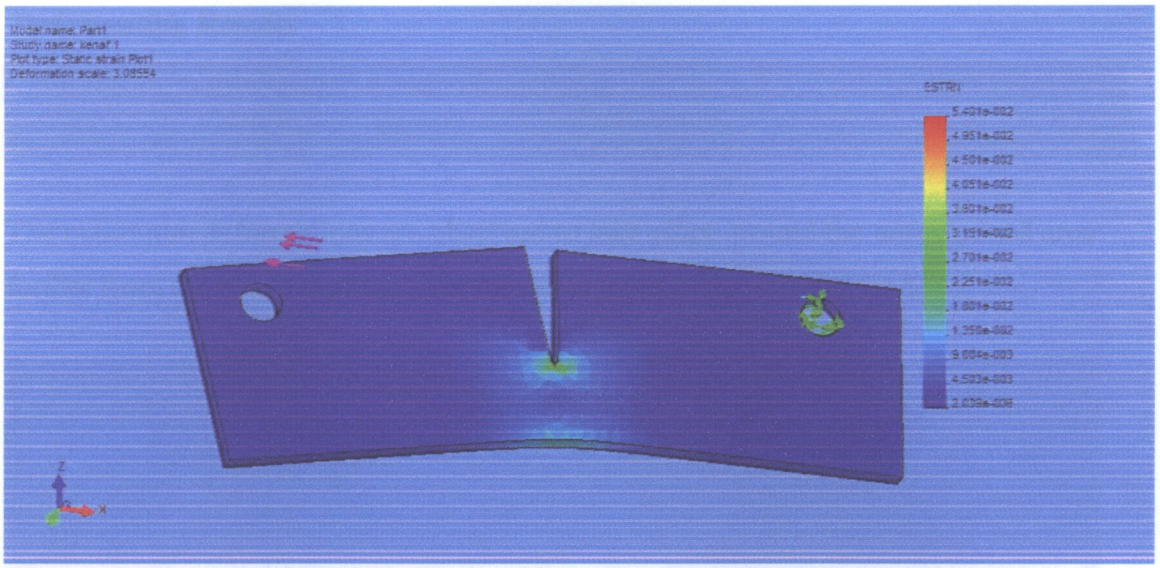

Figure 3.2.2.1.2 Strain results obtained from the simulation

Displacement Results

Name	Type	Min	Location	Max	Location
Plot1	URES: Resultant displacement	0 m Node: 1	(-30 mm, 9.63249e-009 mm, -6 mm)	0.00732472 m Node: 39	(-210.067 mm, 5 mm, 3.85338e-016 mm)

Table 3.2.2.1.7 Shows the values of the maximum and minimum displacement as well as their location on the model

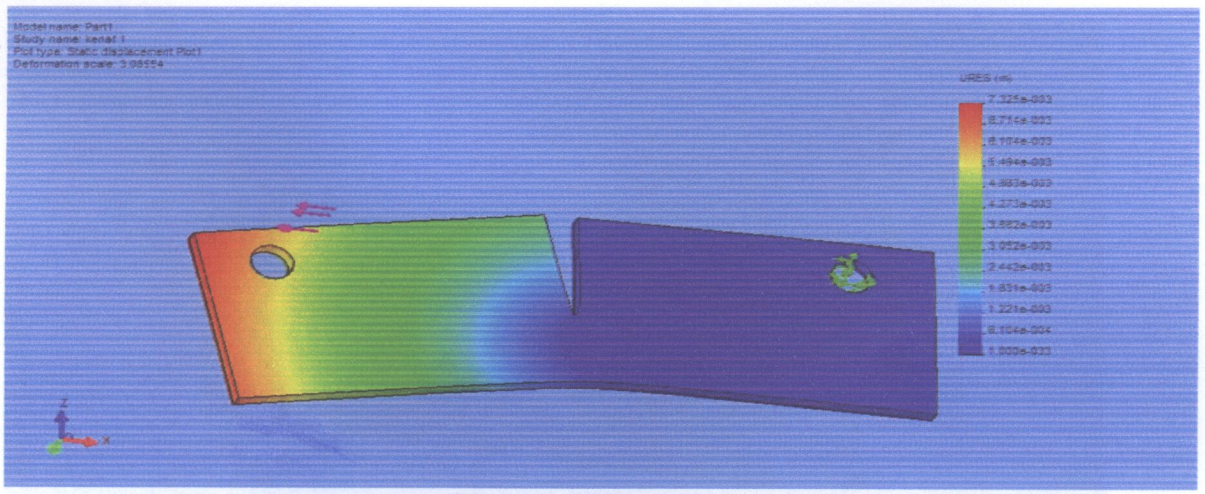

Figure 3.2.2.1.3 Displacement results obtained from the simulation

Deformation Results

Plot No.	Scale Factor
1	3.0855

The maximum deformations are observed to take place around the unrestrained area further from the notch near the point of application of the applied load.

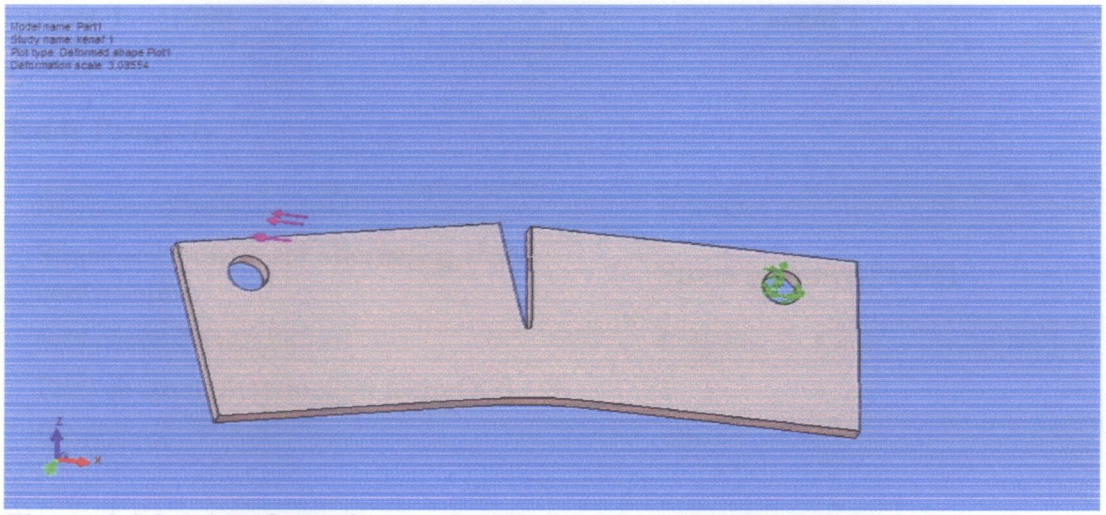

Figure 3.2.2.1.4 Deformation results obtained from the simulation

Design Check Results

The Design check shows the factor of safety distribution in the model if it was not to fail. The maximum factor of safety is found to be around the notch and is about 200.

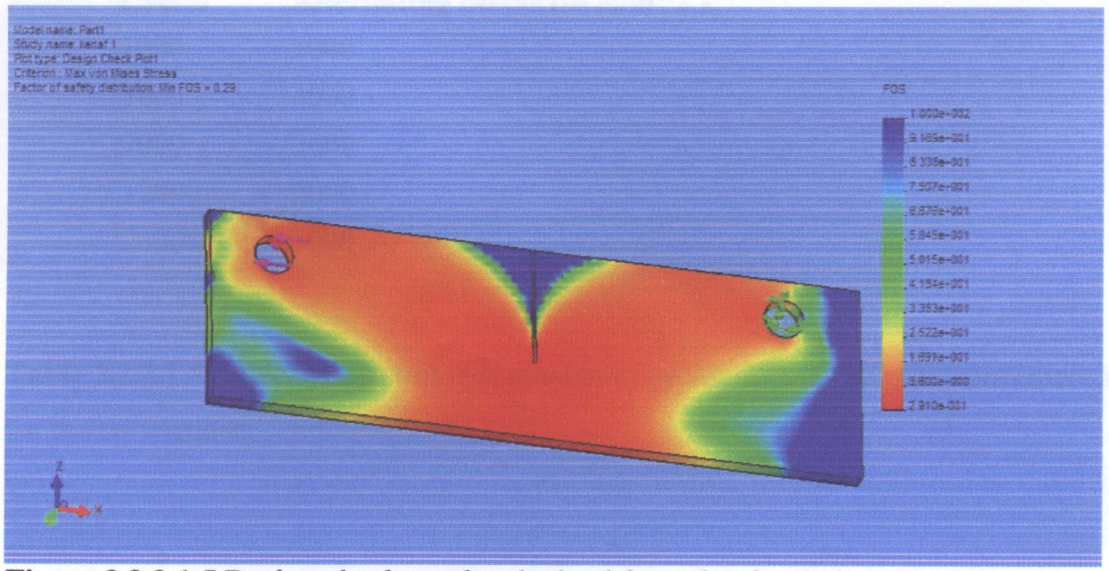

Figure 3.2.2.1.5 Design check results obtained from the simulation

Fatigue analysis

Table 3.2.2.1.8 Below shows the fatigue loading and some fatigue study properties that were applied to the model.

Loading

Name	No. of cycles	Loading ratio(LR)	Study(s)
Event-1	1000	-1	kenaf 1

Study Property

Interaction between event	**Random**
Stress component for alternating stress computation	**Stress intensity(P1-P3)**
S-N curve interpolation	**Log-log**
Fatigue strength reduction factor(Kf)	1
Shell face	Top

Alternating stress vs. Cycles

Data Points:

Cycles	Alternating Stress (in N/m^2)
1000	5000
3000	4000
7000	3000
12000	2000
20000	1000

Table 3.2.2.1.9 Alternating stress vs. number of cycles data points that were entered for the simulations.

Results

Table 3.2.2.1.10 Shows the values of the maximum and minimum damage, factor of safety, the Biaxiality indicator and the life plot as well as their location on the model.

Name	Type	Min	Location	Max	Location
Plot1	Damage Plot	1 Node: 1	(-30 mm, 9.63249e-009 mm, -6 mm)	1 Node: 1	(-30 mm, 9.63249e-009 mm, -6 mm)
Plot2	Life Plot	1000 Node: 1	(-30 mm, 9.63249e-009 mm, -6 mm)	1000 Node: 1	(-30 mm, 9.63249e-009 mm, -6 mm)
Plot3	Factor of Safety Plot	1.99854e-005 Node: 10791	(-108.559 mm, 0 mm, -36 mm)	0.782526 Node: 287	(-206.219 mm, 0 mm, -60 mm)
Plot4	Biaxiality indicator plot	-0.999971 Node: 4492	(-202.372 mm, 0 mm, -27.8209 mm)	0.992819 Node: 10222	(-8.07468 mm, 5 mm, -58.125 mm)

Figure 3.2.1.1.6 Below shows the damage plot of the specified fatigue events

Figure 3.2.2.1.6 below shows the damage plot of the specified fatigue events.

The results for the damage factor indicate that the specified events consume over 100% of the life of the model. Hence the model is considered damaged after applied the specified loads

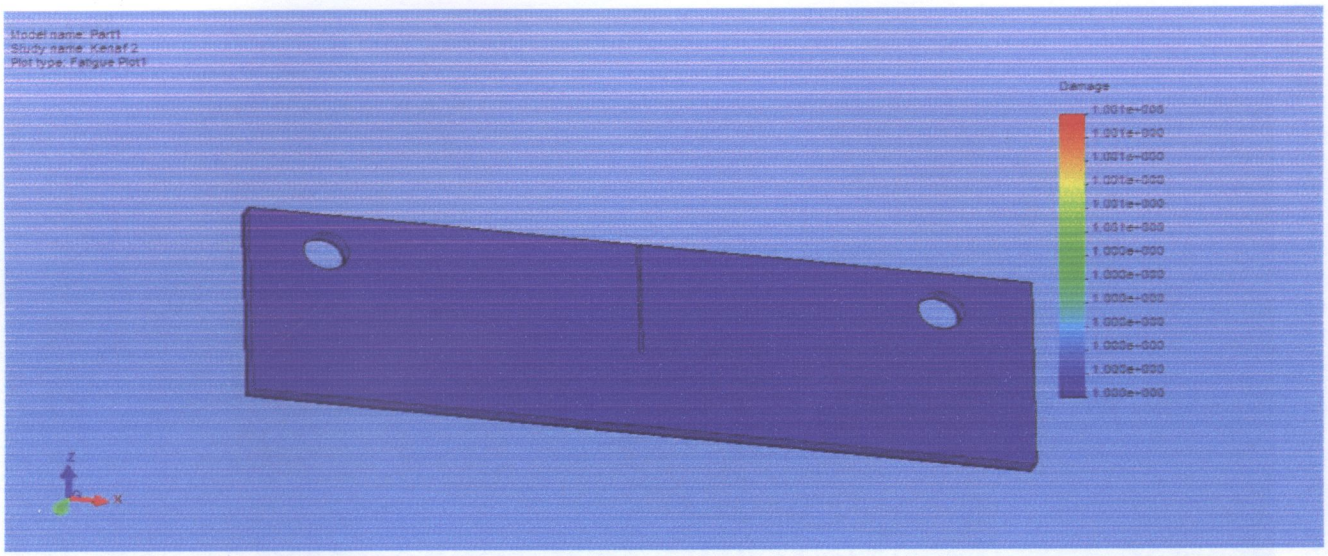

Figure 3.2.2.1.6 Damage plot

Figure 3.2.2.1.7 Below shows the life plot of the specified fatigue events

The life plot shows that failure due to fatigue is likely to occur at the two holes after about 300 cycles

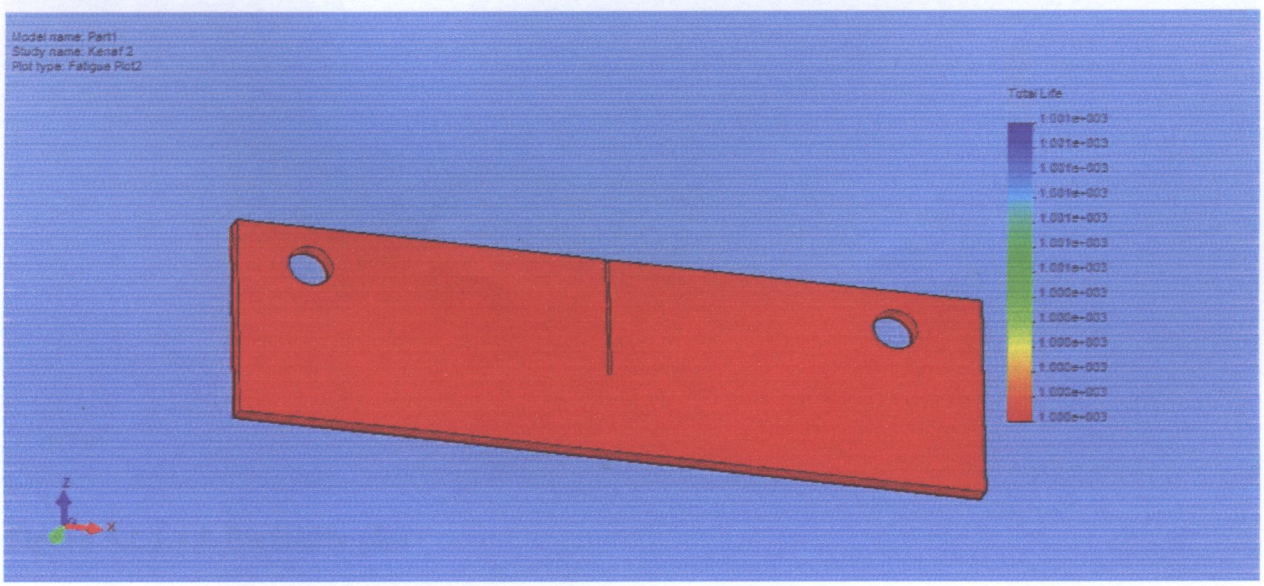

Figure 3.2.2.1.7 Life plot

Figure 3.2.2.1.8 Below shows the factor of safety plot of the specified fatigue events.

The factor of safety results indicate that the model will fail due to fatigue if the current loads are multiplied by 2.0×10^{-5} (the minimum factor of safety). Since the factor of safety is less than one i.e. (factor of safety<1) our model has already failed. Therefore for our model not to fail we need to multiply the loads current by less than 1.9×10^{-5}.

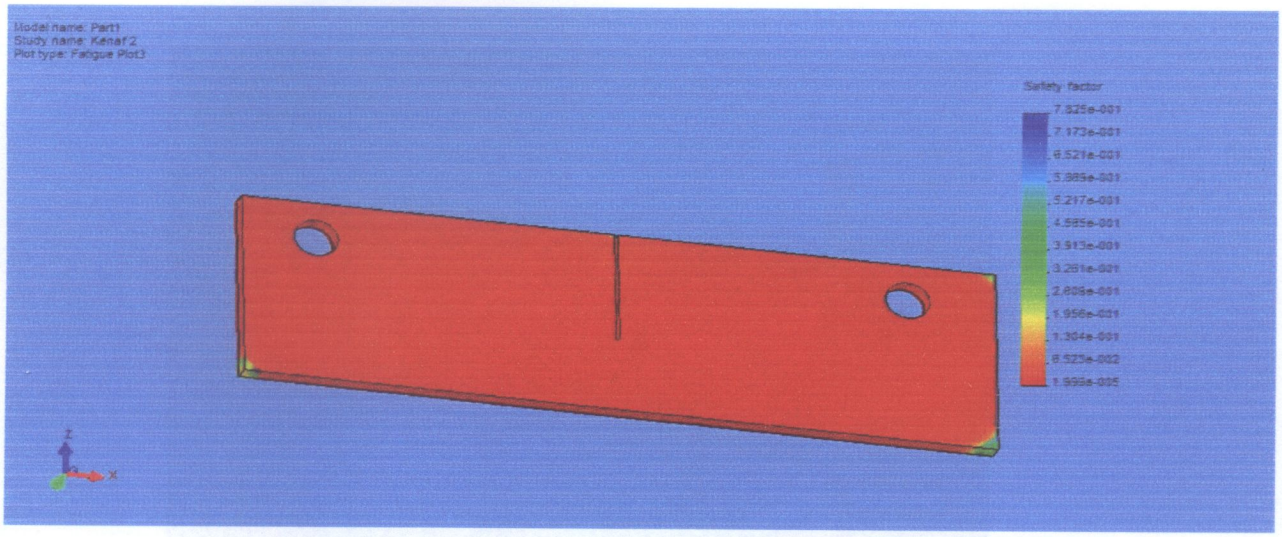

Figure 3.2.2.1.8 Factor of safety plot

Figure 3.2.1.1.8 Below shows the Biaxiality plot of the specified fatigue events.

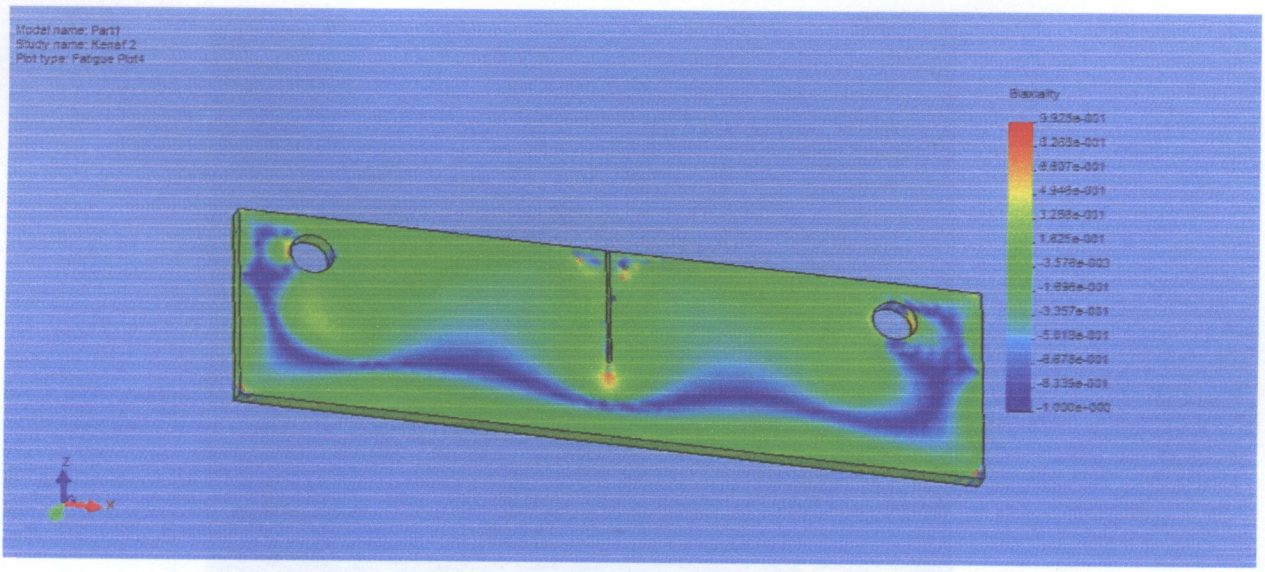

Figure 3.2.1.1.8 Biaxiality plot

3.2.3 Fatigue Simulation of polyester (Lyandenga p 2008)

The results shown in the figure below are fatigue results of polyester material which were obtained after exposing the material to a force of 1 KN, a temperature of 298 K, and number of cycles of 10000 cycles. This was with a dwell time of 20 seconds with a fixed increment of 2 seconds. The dwell time was low because it was taking a long time to run the simulation if a long dwell was chosen. These simulations were done by Lyandenga patience in 2008.

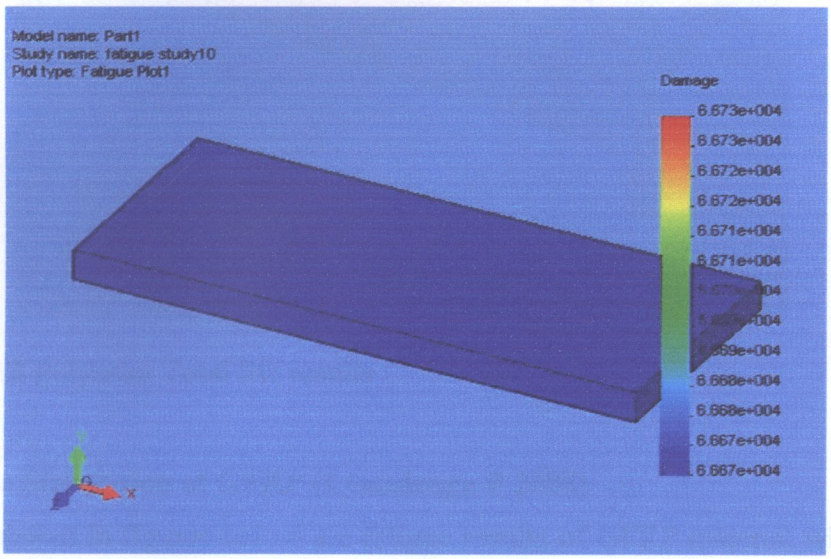

Figure 3.2.3.1 Polyester Fatigue Damage result

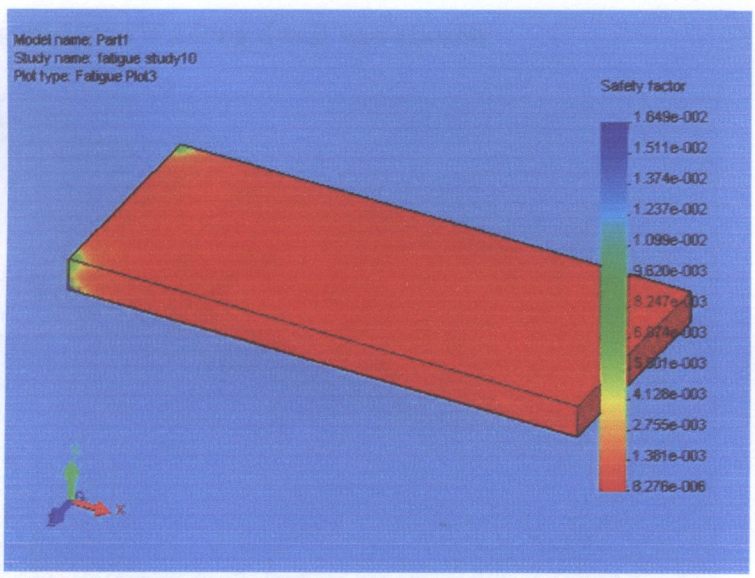

Figure 3.2.3.2 Polyester Safety of factor results

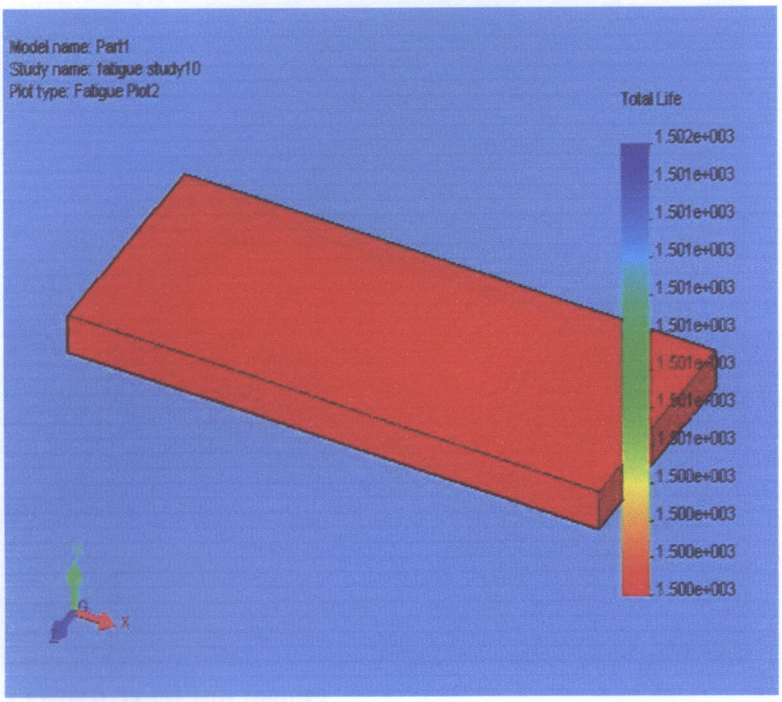

Figure 3.2.3.3 Polyester Total life results

3.2.4 Fatigue Simulation of GFRP (Lyandenga P 2008)

The results shown in figures below are fatigue results of GFRP material which were obtained after exposing the material to a force of 150 KN, a temperature of 373 K, and number of cycles of 10000 cycles. This was with a dwell time of 20 seconds with a fixed increment of 2 seconds. The dwell time was low because it was taking a long time to run the simulation if a long dwell was chosen.

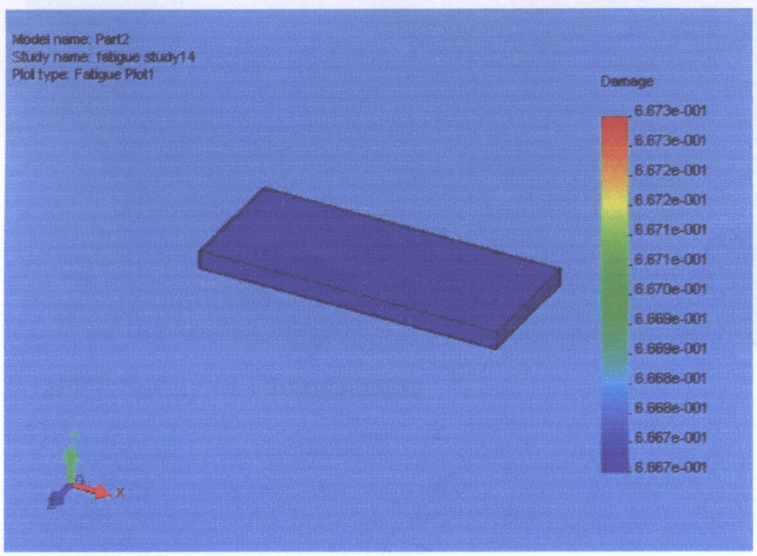

Figure 3.2.4.1 GFRP damage results

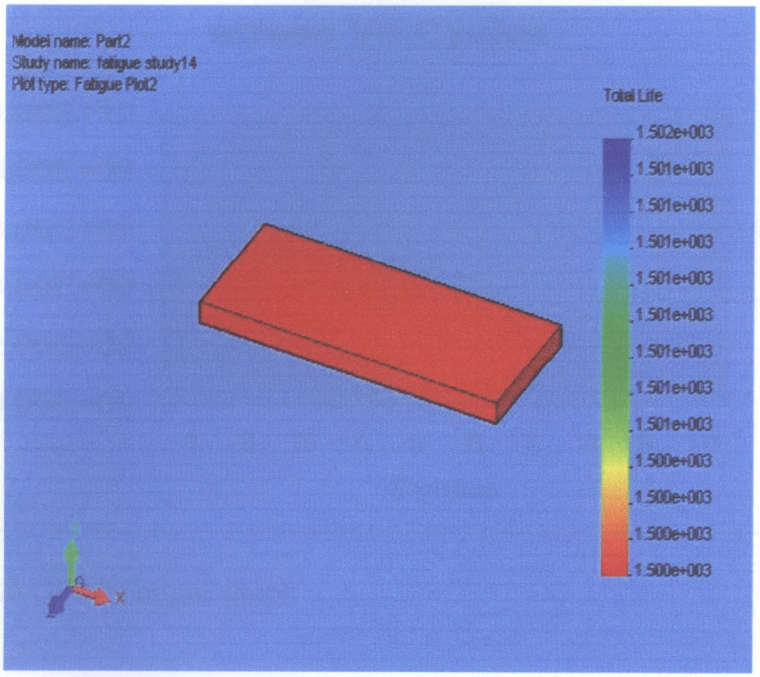

Figure 3.2.4.2 GFRP Total life results

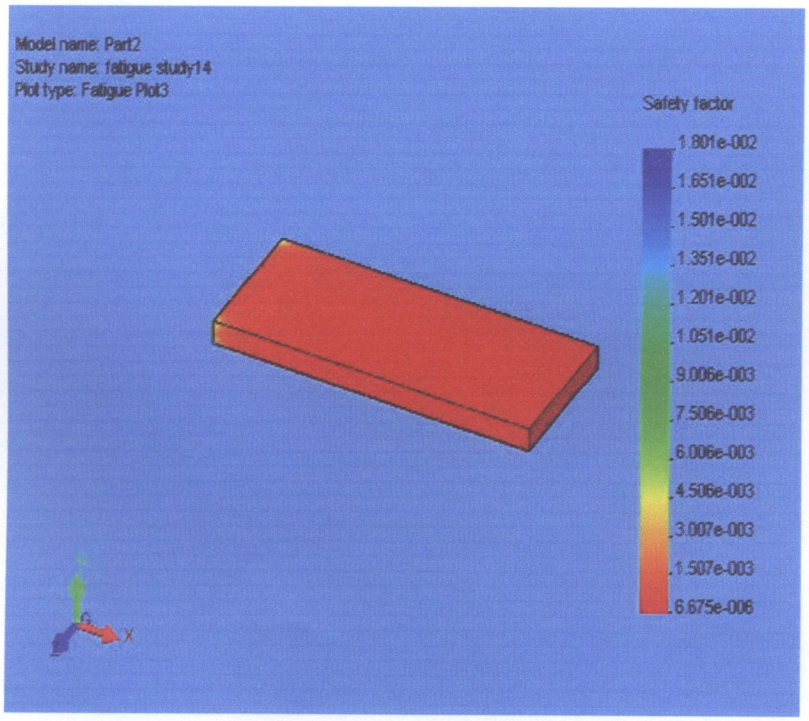

Figure 3.2.4.3 GFRP Safety of Factor results

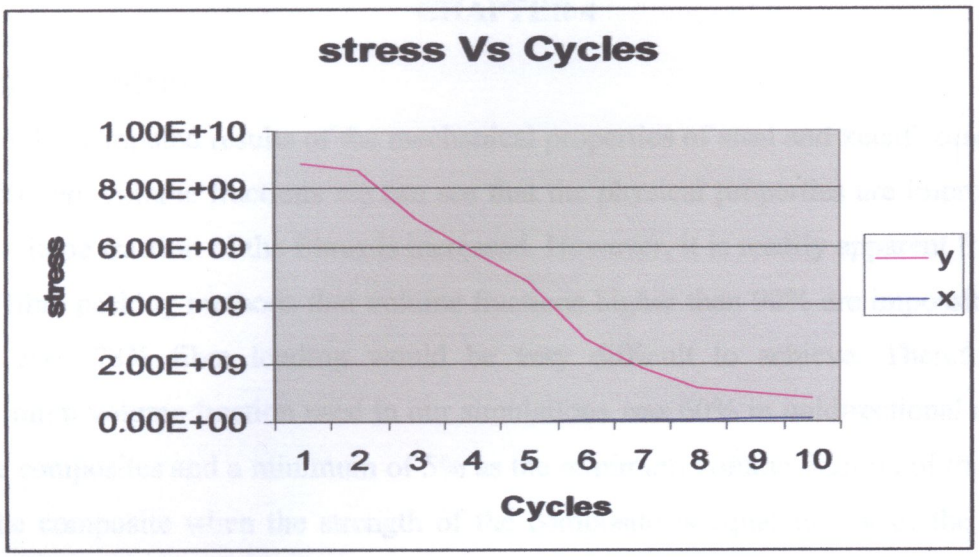

Figure 3.2.4.4 GFRP Fatigue graph

CHAPTER 4

4.0 DISCUSSION

From the computed results of the mechanical properties of sisal and kenaf composites at different volume fractions we can see that the physical properties are improved as the volume fraction of the fibres is increased. However, it is readily apparent from the two fibre packing methods that volume fractions higher than 90% are impossible and that even 78% fibre loading would be very difficult to achieve. Therefore the maximum volume fraction used in our simulations was 60% in unidirectional aligned fibre composites and a minimum of 5% as the minimum volume fraction of the fibres in the composite when the strength of the composite is equal to that of the matrix alone were found to be f=0.0187 and f=0.1 for sisal and kenaf reinforced polypropylene respectively.

From the simulation results for sisal reinforced polypropylene and volume fraction f=0.2, the maximum stresses were observed to take place around the notch as it is a point of stress concentration. Its value was found to be 1200Mpa and the minimum stress on the model was found to be 24.7Kpa. The yield strength was found to be 550Mpa. We see that there is improvement in the value of the yield strength after reinforcing the matrix from 96Mpa and this new yield strength compares well with GFRP which is in the range 450Mpa-800Mpa depending on the volume fraction of the fibres in the composite. The maximum strain was also observed around the notch. The maximum displacements and deformations were observed to take place around the unrestrained area further from the notch. From the design check showing the factor of safety distribution in the model the maximum factor of safety was found to be around the notch and about 200.

The fatigue analysis results for sisal reinforced polypropylene and volume fraction of 0.2 shows that over 100% of the life of the model was consumed as indicated by the damage factor. This meant that the specified events were too much for the model to withstand. The factor of safety results indicate that the model would fail due to fatigue if the current loads were multiplied by 1.726×10^{-5} (the minimum factor of safety). Since the factor of safety was less than one i.e. (factor of safety<1) our model has already failed. Therefore for our model not to fail we needed to multiply the current loads by less than 1.726×10^{-5}.

From the simulation results for kenaf reinforced polypropylene and volume fraction f=0.2, the maximum stresses were observed to take place around the notch also. Its value was found to be 240Mpa and the minimum stress on the model was found to be 5.62Kpa. The yield strength was found to be 110Mpa. We see that there is improvement in the value of the yield strength after reinforcing the matrix from 96Mpa and this new yield strength compares quiet well with GFRP which is in the range 450Mpa-800Mpa. This depends on the volume fraction of the fibres in the composite. The maximum strain was also observed around the notch. The maximum displacements and deformations were observed to take place around the unrestrained area further from the notch. From the design check showing the factor of safety distribution in the model the maximum factor of safety was found to be around the notch and about 200.

The fatigue analysis results for sisal reinforced polypropylene and volume fraction of 0.2 shows that over 100% of the life of the model was consumed as indicated by the damage factor. This meant that the specified events were too much for the model to withstand. The life plot shows that failure due to fatigue is likely to occur at the two holes after about 300 cycles due to the specified loading conditions. The factor of safety results indicate that the model would fail due to fatigue if the current loads were multiplied by 2.0×10^{-5} (the minimum factor of safety). Since the factor of safety was less than one i.e. (factor of safety<1) our model has already failed. Therefore for our model not to fail we needed to multiply the current loads by less than 1.9×10^{-5}.

Comparing the results for sisal and for kenaf reinforced polypropylene with a volume fraction of 0.2 each we can see that sisal improves the physical properties of the matrix more compared to kenaf as can be seen from the tensile strength, the yield strength and the modulus found. This is due to the fact that sisal has a higher tensile strength and modulus as compared to kenaf.

The results from Lyandenga patience were he did simulations on fibre glass reinforced polyester compare well with our simulations of sisal and kenaf reinforced polypropylene meaning that NFRP could be an alternative to GFRP which are very expensive and not locally available. GFRP also have a disadvantage of not be biodegradable

CHAPTER 5

5.0 CONCLUSSION

It can be concluded that NFRP like any other engineering material fails due to fatigue. Simulations for fatigue were successful done and results obtained. But these results needed to be compared with the actual experimental result because simulation results on their own need verification before they could be relied upon. Comparison with experimental results was not possible because the company (Kazuma) that made specimens did not have polypropylene resin from which the composite could have been made.

Nevertheless, the objective of this project were achieved i.e. simulation of fatigue failure in NFRPs (sisal and kenaf) using CosmosWorks. Because the results compare well with those of fibre glass sisal and kenaf could be used as an alternative for the reinforcement since they can readily be available in Zambia as the conditions for their cultivation are favourable due to good climate and the availability of good arable soils. Sisal and Kenaf are also biodegradable.

5.1 RECOMMENDATION

1. Since the results from the simulations compares well with those of fibreglass, NFRP could be an alternative in the boat industry, automobile industry for car bodies, water tanks and for garden hoses. However, if they are to be use for making transparent roofing sheets experiments should be carried out to determine if it is possible to decolour the fibres such the composite could be transparent.
2. Once industries that will be using natural fibres are set up, there is need to encourage local farmers to start farming sisal and kenaf as the conditions for their cultivations are favourable (good soils and climate) in Zambia.

RERERENCES

1. Ashby, M. F, and D.R.H Jones(1980), "Engineering Materials I", New yolk: Pergamon Press,

2. McCrum, N. G (1997), "Principles of Polymer Engineering" New York: Oxford University Press.

3. Dieter George E. (1998) "Mechanical Metallurgy", London: McGraw-Hill Company.

4. Chikampa Sydney (2008) "Investigation of creep-fatigue failure in Glass-fibre reinforced polymers" Final year project report, Lusaka: University of Zambia, Unpublished.

5. Lyandenga Patience (2008) "Simulation of creep-fatigue failure in Glass-fibre reinforced polymers" Final year project report, Lusaka: University of Zambia, Unpublished.

6. Rajput, R. K. (2004) "Engineering Materials)", Revised Edition, New Delhi: S. Chand & Company Ltd.

7. William, Jr, D. C (2005) "Materials Science and Engineering an introduction", Sixth Edition, New York: John Willey & Sons (Asia) Pte Ltd.

8. Collins J.A (1981) "Failure of materials in mechanical design: Analysis, prediction and prevention", New York: Willey interscience publication.

9. Crawford R.J (1985) "Progress in polymer science, Volume 7: Plastic engineering", Oxford: Pergamon press.

10. Sonat F, "Mechanical characterisation" at www.biomed.metu/edu.tr/courses/tem-papers

11. Cai, Changan, Liaw, Peter K, Ye, Mingliang, and Yu, Jie, "Mechanical overview" at www.tms.org.

12. Rowell el al (1999) "Kenaf Properties, Processing and Products" Mississippi State University, Ag & Bio Engineering

13. Herzberg R.W and Manson J.A, (1980) "Fatigue of Engineering Plastics", London: Academic Press.

14. Suresh S. (1998), "Fatigue of Materials", 2nd Edition, London: Cambridge University Press.

15. Sullivan P (2003), "Kenaf Production" NCAT.

16. Zoltán Mezey, (1997) "Investigation of the mechanical properties of sisal fiber reinforced polypropylene composites" Budapest University of Technology and Economics, Hungary.

17. Kuruvilla Joseph, (1997) "A Review on sisal fibre reinforced polymer composites" Oxford.